Elsevier Editorial System(tm) for Surface and Coatings Technology

Manuscript Draft

Manuscript Number: SURFCOAT-D-18-02222R1

Title: Cathodic Discharges During High Frequency Plasma Electrolytic Oxidation

Article Type: Full Length Article

Keywords: plasma electrolytic oxidation; cathodic discharges; high speed photography.

Corresponding Author: Professor Trevor William Clyne, PhD

Corresponding Author's Institution: Cambridge University

First Author: Sam C Troughton, MSci (Cantab)

Order of Authors: Sam C Troughton, MSci (Cantab); Trevor William Clyne, PhD

Abstract: Using small area electrical data logging, high speed photography, sample mass gain monitoring, gas evolution measurement and microstructural examination, a study has been made of the formation and effect of cathodic discharges during PEO of Al substrates. Discharge formation during the cathodic half-cycle is promoted by high frequency, thick coatings and high pH. They form (under constant current conditions) when the voltage during cathodic polarization reaches a value (~250 V in the work described here) sufficient to cause dielectric breakdown across thin residual oxide layers on the substrate. This occurs when the normal cathodic process of proton flow through electrolyte channels in the coating can no longer deliver the required current. Cathodic discharges tend to carry higher currents, and emit more light, than anodic ones. Gas evolution rates during PEO are well above the Faraday yield level. This is due to water entering discharge plasmas, breaking down into ionized species and failing to recombine completely during subsequent collapse and quenching. It is reported here that rates of gas evolution rise as discharges start to take place in the cathodic part of the cycle, as well as in the anodic part. Rates of substrate oxidation (coating growth), however, drop off, rather than rise, when cathodic discharges start. Evidence is presented here suggesting that this is associated with their highly energetic nature, causing substantial amounts of oxide to be expelled into the electrolyte during cathodic discharges. This is also apparent in the coating microstructure, where recent cathodic discharge sites are identifiable as large, highly porous regions.

Research Data Related to this Submission

There are no linked research data sets for this submission. The following reason is given:
Data will be made available on request

University of Cambridge
Department of Materials Science & Metallurgy

27 Charles Babbage Road
Cambridge CB3 0FS

Prof TW Clyne FREng
Professor of Mechanics of Materials
Director of Gordon Laboratory
Helmholtz International Fellow

office 0044 1223 334332
lab 0044 1223 334340
reception 0044 1223 334300

twc10@cam.ac.uk
www.ccg.msm.cam.ac.uk/

Allan Matthews
Editor
Surf. Coat. Techn.

14th Aug. 2018

Cathodic Discharges During High Frequency Plasma Electrolytic Oxidation

SC Troughton & TW Clyne

Dear Allan

Following the comments of the two reviewers, I'm submitting a revised version of this paper, together with a response document.

Best Wishes

Bill

14th Aug. 2018

"Cathodic Discharges During High Frequency Plasma Electrolytic Oxidation"

SC Troughton & TW Clyne

Reviewer #1

In this paper, the correlation between timings of the polarising signal and discharge phenomenon has been found. Authors demonstrated that the shorter pulses the higher probability of discharge phenomenon under negative polarisation, however, positive discharges were found independent of frequency (50, 2500Hz). Moreover, it was found that at 2500Hz and certain time point the PEO process changes in such a way that gas elaboration substitutes coating growth. Undoubtedly, those observations have direct connection with fundamental mechanism of PEO, in spite of coating degradation under particular conditions. Nevertheless, following questions should be clarified before acceptance:

1) *Title and text: Authors used indirect characteristic as "Frequency" instead of pulse and pause durations, later look more suitable for non-harmonic waveforms characterisation. This makes unclear the main factor of those effects. Is it duration of cathodic or anodic pulse? Maybe pauses between them are more important?*

   For all of this work, there is no pause between the anodic and cathodic pulses, and the pulse width ratio is unity throughout. Frequency is thus an appropriate characteristic on which to focus. This has been clarified.

2) *Introduction: "Most of the injected energy eventually goes into heating of the electrolyte (via expansion of a gas bubble centred on the discharge site [10]), with little or no scope for subsequent recovery." It sounds like some part of energy does not transform into a heat. Actually, all injected energy goes into heating of surrounding media. The real heating even higher then injected energy, since it includes energy produced by oxide formation (see ref. 10. Sec.4.5) in addition to injected one.*

   It is correct to state that nearly all of electrical energy does go into heating the electrolyte, and it's also true that there is an additional (small) amount of released energy from the enthalpy of oxidation. However, it is now clear that there must also be a small amount of energy that goes into gas evolution and escapes from the system. This has not previously been considered. It also is relatively small, but it does justify use of the expression "Most of…", rather than "All of..". This has been clarified.

3) *Methodology: Presented manuscript has severe methodological inconsistency. In accordance with Dunleavy et al, the small area experiments mean that particular conditions within large and small areas are expected to be the same. However, experimental results, presented in this manuscript, illustrate violation of that approach. From waveforms, it is clear that particular conditions on large sample and small one are not similar. Smaller sample does not represent part of the larger one:*
a) It can be clearly seen that small area sub-electrode is exposed to extremely high current density (e.g. from Fig.5, 100mA/7.9E-3cm2 = 125A/dm2). Such current density is far from typical values in PEO, this is more similar to plasma assisted material removing (e.g. plasma polishing), where light emission can be observed on a wide range of conducting materials from graphite to stainless steel. Perhaps, "discharges" attributed to smaller specimen, considered in this manuscript (both positive and negative), has little relation to the PEO process.

There seems to be a misunderstanding here. Typical current densities during PEO are in the range of a few tens of A dm^{-2}. A value of 30 A dm^{-2} has been used in this work. However, at least during anodic periods, this current flows in the form of a large number of short duration discharges distributed over the surface of the sample. Each discharge carries a current of a few tens to hundreds of mA (for periods of the order of a hundred μs). The current of 100 mA on the small area sample relates to a period during which there was an active discharge, as confirmed by light emission. It therefore represents an individual discharge current. Discharges are not necessarily active during every half-cycle, due to the stochastic nature of the dielectric breakdown, and there may be extended periods without any discharges or significant current flow occurring on the small area sample (or indeed in any particular region of a large sample). This kind of behaviour can be seen more clearly in Fig.2(b) for 50 Hz, where there are peaks in the small area current (up to 100 mA), but a relatively low baseline current during periods with no active discharges. After extensive investigation over a number of years, we feel that there is overwhelming evidence that data obtained from small area samples provide valuable information about how PEO takes place on a real (large area) sample. It is, however, recognized that the average current density on a small area sample may differ slightly from that on a large area one (due to what might be described as "edge effects"). This has been clarified.

b) It is known that PEO load has RC behaviour for positive and RL behaviour for negative polarisations. Additional resistor (100 Ohm current sensor) was included between power source and capacitive load (small sample), whereas large sample had direct connection. There is no reason to expect any similarity in such system especially taking into account sever non-linear response of PEO load. In order to have reproducible results it is more suitable to use contactless current sensor (based on hall effect, for instance) rather than current shunt, which adds voltage drop (see below). Moreover, Dunleavy et al. employed current transformer in his original experiments that is not ideal, but much precise.

There will indeed be a small load (voltage drop) across this resistor, but this will have only a small effect with regard any difference between measured and actual voltages acting on the sample. It is also felt that any changes in the capacitive or inductive characteristics of the system due to the presence of this resistor will be small.

c) The coupling (100 Ohm) resistor is too large for this purposes. If current density had the same values for large and small electrodes, the absolute current value on small electrode would have ~2.4mA and corresponding voltage drop on the resistor would have 240mV. It is much smaller than +600V or -250V and could be neglected. However, in real experiments, current spikes reached 100-200 mA (Fig.4,5). As a result, voltage drop on current shunt appears to be 10-20 Volts. Taking into account severe non-linear dependence of current on applied voltage for the PEO load, we have to conclude that current will drop considerable, violating similarity of the conditions within large and small areas. In order to have reproducible electrochemical processes on both specimens they definitely should have equipotential connections.

The point is in general well-taken, but, as outlined above, the overall effect of this on the measured characteristics will be small. This has been clarified.

4) *It looks unexpectedly that so different frequency produced quite similar coating morphology. Normally, the higher frequency the smaller size of structural elements of the coatings (craters, bubbles etc.).*

The present study has not specifically involved detailed characterization of the coating microstructure.

5) *From the fact that smaller specimen had different electrical conditions in respect to larger one. It is incorrect to discuss coatings' feature on large sample with connection to light emission from the smaller one. The current densities were very different*

As outlined above (point 3)), it is not correct to state that the current densities on small area and macroscopic samples were "very different", although it is accepted that they were not exactly the same. All microstructural features have been identified on bulk samples of Al-1050, and distinct light emission events occurred on these samples under cathodic polarisation – which is the source of the data in Fig. 7 relating to the number of anodic and cathodic discharges

Reviewer #2

The authors reported the detection of cathodic discharges during PEO under high frequency, however, I feel that the cathodic discharges may be not the true cathodic discharges. The light emission may be from the unquenched discharge channels. Hence, it is suggested that the authors provide more evidence to confirm the existence of cathodic discharges.

In fact, the evidence that cathodic discharges were occurring is overwhelming. Extensive previous work with small area samples has shown that flow of current within a discharge (through a plasma column) coincides exactly with the associated light emission, at least to within a few μs. (There is no significant "after-glow".) There is also no question that, under certain conditions, (small area) current flow and simultaneous light emission can occur during the cathode half-cycle. In fact, it's also clear that, when both anodic and cathodic discharges are occurring simultaneously on the same (small) sample, they tend to be in different locations. There is simply no possibility that the observed cathodic discharges are in reality anodic discharges. Of course, cathodic discharges do occur only under certain conditions, as outlined in the paper.

This paper reported the recording of cathodic discharges under plasma electrolytic oxidation (PEO) of a 6082 Al alloy at high frequency (2.5 KHz) and the relationship of the cathodic discharges with the coating thickness and microstructure. In my opinion, the cathodic discharge is still a topic of controversy in PEO study, and hence the authors should be careful to reach their conclusions in this paper. The authors reported that cathodic discharges happen when the cathodic voltage reaches ~250 V. However, it is evident that the same voltage value cannot cause the dielectric breakdown of the initial oxide layer if the PEO was carried out under anodic polarization. How can dielectric breakdown of a thick coating occur under a much lower voltage? Detailed comments are listed below:

It is now well established that (for both anodic and cathodic discharges), the actual dielectric breakdown occurs, not across the coating as a whole, but across a thin oxide layer at the root of a pore (column of electrolyte). This explains a number of features, including the fact that the breakdown voltage tends to remain approximately constant while the coating thickness increases. It does appear that a rather different voltage is required to stimulate cathodic discharges, compared with that for anodic discharges, but this is not really surprising.

1) *Page 4, section 2.1: "For high speed video, synchronised with electrical monitoring, the samples employed were Al-6082 substrates,"- However, in the experimental section 2.3, it is said that Al-1050 was used for monitoring gas evolution and mass gains. Is it true that two kinds of Al alloy are used in the study?*

   This is correct. It has been confirmed that, at least as far as cathodic discharges are concerned, the two alloys behave similarly.

2) *Page 4: "The high speed camera generated a TTL trigger signal (+5 V, 10 <mu>s square wave) within 100 ns of the camera being activated."- Could you provide the full name of "TTL" and the waveform of the trigger signal? Was there an interval between two images (frames)? Could you provide more details about how the current signal and video recording was monitored synchronously?*

   "TTL" refers to a Transistor-Transistor-Logic signal - this is a common signal used in electronic controls. The meaning of the acronym has now been clarified. The camera outputs a single square wave pulse, rising from 0 V to +5 V and back to 0 V with a duration of 10 µs. The oscilloscope has one channel monitoring the camera TTL output, and recording is triggered by the rising edge of the TTL signal. The camera frame rate was 125,000 frames per second. There is a negligible dead time between frames (the actually exposure is fractionally shorter than 8 µs). These details have been clarified.

3) *Page 7, a typo exists in the sentence: "These started to form only after the after the coating thickness had reached about 30-40 <mu>m."*

   This has been corrected.

4) *In my opinion, the observation of the discharges at the cathodic half-cycle does not necessarily mean that the discharges are "cathodic discharges". The "cathodic discharges" are possibly an extension of the preceding anodic discharges, since light emitting from the discharge channels may not be stopped instantly after the cut-off the anodic current. Discharge channels in thick coatings are more difficult to cool down, which may be why "cathodic discharges" are observed with thick coatings.*

This point is addressed above.

5) *It is suggested that the authors monitor the discharge behavior under unipolar waveforms (without cathodic current) at high frequency to see if there are any light emissions at the pulse-off duration. The detection of light emission at positive pulse-off duration will confirm the above speculation*

This is unnecessary in view of the above responses.

6) *Section 5.1, "To produce the oxygen present in the coating, water must be decomposed, causing hydrogen gas to be released."- Electrochemically, the gas generated on the anode should be oxygen, not hydrogen. There is a mistake in your estimation.*

It is important to appreciate that PEO is not a conventional electro-chemical process. This is clear from the fact that gas evolution rates routinely exceed the Faraday yield level. The main source of the oxygen that goes into creation of the metal oxide is H_2O that has entered the plasma and dissociated. This leaves an excess of hydrogen in the plasma, which is likely to be released as molecular hydrogen gas. In fact, even if the amount of oxygen extracted from the plasma by reaction with metal (during cooling) is small, it is possible that recombination of hydrogen and oxygen may be incomplete, so that gas evolution could occur.

***Highlights (for review)**

- High speed video and electrical monitoring of discharges in PEO
- Confirmed conditions and mechanisms that promote cathodic discharges
- Correlation with microstructural effects

Re-submitted to Surf. Coat. Techn., Aug. 2018

CATHODIC DISCHARGES DURING HIGH FREQUENCY PLASMA ELECTROLYTIC OXIDATION

SC Troughton & TW Clyne[*]

Department of Materials Science & Metallurgy
Cambridge University
27 Charles Babbage Road
Cambridge CB3 0FS, UK

Abstract

Using small area electrical data logging, high speed photography, sample mass gain monitoring, gas evolution measurement and microstructural examination, a study has been made of the formation and effect of cathodic discharges during PEO of Al substrates. Discharge formation during the cathodic half-cycle is promoted by high frequency, thick coatings and high pH. They form (under constant current conditions) when the voltage during cathodic polarization reaches a value (~250 V in the work described here) sufficient to cause dielectric breakdown across thin residual oxide layers on the substrate. This occurs when the normal cathodic process of proton flow through electrolyte channels in the coating can no longer deliver the required current. Cathodic discharges tend to carry higher currents, and emit more light, than anodic ones. Gas evolution rates during PEO are well above the Faraday yield level. This is due to water entering discharge plasmas, breaking down into ionized species and failing to recombine completely during subsequent collapse and quenching. It is reported here that rates of gas evolution rise as discharges start to take place in the cathodic part of the cycle, as well as in the anodic part. Rates of substrate oxidation (coating growth), however, drop off, rather than rise, when cathodic discharges start. Evidence is presented here suggesting that this is associated with their highly energetic nature, causing substantial amounts of oxide to be expelled into the electrolyte during cathodic discharges. This is also apparent in the coating microstructure, where recent cathodic discharge sites are identifiable as large, highly porous regions.

Keywords: plasma electrolytic oxidation; cathodic discharges; high speed photography.

1 Introduction

Interest in Plasma Electrolytic Oxidation (PEO) continues to grow, and the technical attractions of the process are well established, but the mechanisms of oxide growth remain quite poorly understood. The key to improved understanding certainly lies in detailed study of the individual discharges, and indeed considerable progress has been made recently as a result of such investigations [1-8]. It's now clear that discharges have a strong tendency to occur in sequences ("cascades") at particular locations, with each

[*] tel: 0044 1223 334332: e-mail: twc10@cam.ac.uk

discharge being of relatively short duration (few tens to few hundred μs), but the periods between them are somewhat longer (several hundred μs to a few ms) and the cascades can persist over many cycles of the applied potential. It's also clear that the process exhibits low energy efficiency [7, 9, 10], with relatively large amounts of electrical energy (~1 mJ) being absorbed during a discharge, each of which results in the creation of only a small amount of oxide (< 1 ng). Most of the injected energy eventually goes into heating of the electrolyte (via expansion of a gas bubble centred on the discharge site [10]), with little or no scope for subsequent recovery. (A small amount of energy is carried away in the form of evolved gas.) However, this high rate of energy absorption is not necessarily inherent in the process and further improvements in understanding of how each discharge arises may lead to technological and economic benefits. Some efforts have been made in the direction of measures to reduce energy absorption during the process, such as the suggestion of Zhang et al [11, 12] that a grid counter-electrode should be located close to the surface of the substrate, but these have not so far been formulated within a well-defined theoretical framework or been widely adopted.

An issue that is receiving increasing attention concerns the significance of the cathodic part of the cycle. It's been clear for some time [13] that PEO coatings produced using AC are in general of superior quality (harder and denser, for example) than those produced under corresponding (anodic) DC conditions. It's also been shown that coating quality is improved if the cathodic voltage is raised [14] or if the ratio of cathodic current to anodic current is increased [15]. What actually happens during the cathodic half-cycle is less clear. It's certainly the case that, at least under most conditions, discharges predominantly occur during the anodic half-cycle, although current does flow in both half-cycles.

However, discharges have been observed in the cathodic part of the cycle under some conditions, usually after the coating has become relatively thick. Rakoch et al [16] reported that such discharges are favoured by more acidic electrolytes, relating this to the rapid acceleration of protons (towards the substrate) during the cathodic part of the cycle, bombarding the thin film of oxide on the substrate and hence making it more likely that it will undergo dielectric breakdown. On the other hand, Sah et al [17] reported that cathodic discharges tend to occur in strongly alkaline (silicate) electrolytes, and can improve the coating quality. Nominé et al [18-20] reported that high pH, and also high supply frequency and greater coating thickness, favour cathodic discharges.

It is not immediately clear whether having a high H^+ ion concentration is in fact expected to promote or inhibit cathode discharges. Certainly the argument of Rakoch et al [16] does not explain the observation that they tend to occur with relatively thick coatings. Possibly a useful approach is to recognize that, when there is a high H^+ ion concentration, and only a short column of electrolyte above the thin oxide layer on the substrate (ie a thin coating), then plenty of H^+ ions reach the layer (during the cathodic part of the cycle), pick up electrons that are coming through the layer and form H_2 gas. However, a shortage of H^+ ions (high pH), a long distance through the electrolyte column (thick coating) and a short cathodic period (high frequency) are all likely to make this

process more difficult, causing the current carried by the H^+ ions to fall, the voltage to rise (in order to maintain the current at the set value) and, when a sufficiently high field is thus created across the oxide layer, to cause dielectric breakdown. This explanation does not appear to have been put forward previously, although it should be recognized that the exact outcome is likely to depend on the details of the electrical circuitry.

Nomine et al [19] reported that cathodic discharges on Mg tend to be detrimental to the coating microstructure, although having a cathodic voltage is beneficial and they speculate that this relates to the associated charge redistribution somehow making the anodic discharges more effective. It's also worth noting that PEO coatings have been produced under conditions in which cathodic discharges predominate. For example, Stojadinovic et al [21] reported cathodic PEO of Mo. Recognizing that coating creation (substrate oxidation) during PEO predominantly occurs during cooling of a plasma containing both substrate atoms or ions and oxidizing agents of some sort [8], it seems likely that this can take place as readily in a cathodic discharge as in an anodic one.

There have been relatively few studies of gas evolution during PEO processing. There is conflicting evidence regarding the composition of the evolved gas, with some reports that it is predominately oxygen [22, 23], and others suggesting high concentrations of hydrogen [24]. It is, however, commonly reported [22-26] that the volume of gas liberated is considerably greater than the electrochemical Faraday yield, corresponding to electrolysis of water. This has also been reported for contact glow discharge electrolysis [27, 28].

In any event, there are evidently several unanswered questions in this area. In practice, PEO processing is commonly carried out using AC supplies at 50 or 60 Hz, although higher frequencies are being increasingly employed. At low frequency, the cycle period is about 20 ms, which is sufficiently long to allow extended cascades during each (anodic) half-cycle - and indeed they commonly persist at the same location through a number of cycles. There is interest in how the process might change as the supply frequency is increased, such that the cycle period is no longer large compared with the inter-discharge period, or the discharge period itself, but there appears to have been little systematic work on this. Yao et al [29, 30] investigated the effect of cathodic pulses over a range of frequency, for PEO of titanium, observing some changes in the phases formed in the coatings, but did not explore any details of the discharges. There are several reports [3, 31-33] that an increase in the supply frequency (with maximum values usually around 1.0-1.5 kHz) leads to a reduction in coating growth rates, as well as a coating microstructure that becomes finer and denser (so that high frequency might be regarded as beneficial in this respect). However, little information appears to be available about how the nature of the (anodic and/or cathodic) discharges might change as the frequency becomes relatively high. The present paper is aimed at this area, as well as at effects on the coating microstructure.

2 Experimental Procedures

2.1 Sample Preparation and PEO Processing

For high speed video, synchronised with electrical monitoring, the samples employed were Al-6082 substrates, in the form of 25.4 mm square section bars mounted in resin. A small piece of the bar was swaged to produce a wire of diameter 1 mm, which was mounted in the resin, adjacent to the bar. The wire and bar were connected to a pair of PVC-insulated twisted wires extending out of the tank, where a 100 Ω resistor connected the ends of the twisted wires. The set-up is described in detail in papers of Dunleavy et al [1, 6]. It allows the current though the small sample to be monitored, and this signal to be synchronised with high speed photography (and, at least in principle, with high speed spectral analysis).

Coatings were prepared using a 100 kW Keronite™ processing rig, with an electrolyte of a dilute aqueous solution of potassium hydroxide and sodium silicate (pH = 11.7), maintained at about 20˚C by re-circulation through a heat exchanger. The applied potential was square-wave and most of the work presented was carried out at either 50 Hz or 2.5 kHz. In all cases, the anodic and cathodic periods were equal, with no gap between them, so that the conditions are fully defined by the frequency. A constant current condition was set, so as to achieve a current density of 30 A dm^{-2}. The applied voltage was therefore not pre-determined, but adjusted by the power supply to maintain the appropriate current, which was about 2.0 A for these samples. Mass gain and microstructural observations were made on standard plates of Al-1050 with dimensions of 50 × 25 × 1.2 mm.

2.2 High Speed Video Capture

The camera employed for synchronized current and video experiments was a Photron FastcamSA 1.1, with the acquisition rate set at 125,000 frames per second (8 μs exposure time). The linear spatial resolution was 9 μm - ie an area of 81 μm^2 per pixel. Typical images comprised 192 × 144 pixels, covering an area of 2.24 mm^2, which was large enough to view the entire cross section of the small area (1 mm diameter) wire. Sample surfaces were viewed through a glass window in the electrolyte tank. The set-up is fully described in a previous paper [10]. In the present work, no illumination was needed, since the images were created only by light emitted from the discharges. Image sequences were acquired after various PEO processing times, using different frequency waveforms. The high speed camera generated a TTL (Transistor-Transistor Logic) trigger signal (+5 V, 10 μs square wave) within 100 ns of the camera being activated. Since each frame corresponds to 8 μs, this 100 ns delay is considered negligible. The trigger signal was connected to one channel of a Picoscope, to initiate electrical recording.

Monitoring of the number of cathodic discharges occurring at various processing times was performed using a Phantom V12.1 camera, with an acquisition rate of 100,000 frames per second (10 μs exposure time). The linear spatial resolution was 34 μm – ie an area of 1156 μm^2 per pixel. Typical images comprised 160 × 160 pixels, covering an

area of 30 mm^2 in the centre of the plates. Recordings were performed throughout processing, in sequences of 173 ms duration.

2.3 Monitoring of Gas Evolution and Mass Gains

Gas evolution is not routinely monitored during PEO processing, although, as outlined above, there have been a few studies. The gas produced is expected to be a mixture of H_2 and O_2, so storing large quantities is potentially hazardous. In addition, compositional analysis of the gas is complicated by the fugitive nature of hydrogen gas, making it rather difficult to handle for analysis purposes. The current work has therefore been limited to measurement of the net gas evolution rates. Furthermore, in order to avoid collecting large quantities, while studying rates over relatively long periods, some special measures were necessary. The gas was therefore collected from a relatively small ("monitoring") sample. However, the processing unit used could not deliver small currents reliably. Therefore, two samples were processed in parallel, with a large shunt sample in addition to the monitoring sample.

The monitoring samples were made of Al-1050, with dimensions of 28 × 10 × 1.2 mm. A wax coating (Suprawax) was applied on one side and around the edges of each sample, leaving an exposed area for processing of 20 × 10 mm. Shunt samples were also made of Al-1050 and had an exposed area of 2,500 mm^2. Samples were processed such that the current flowing through the monitoring sample was ~0.6 A, to achieve a current density of 30 A dm^{-2}. Current flowing through the monitoring sample was measured by making the electrical connection to the bus bar through a 1 Ω resistor. The voltage drop across this resistor was measured using an active differential probe (Pico Technology TA043) with 10× attenuation. The shunt samples used for 50 Hz processing were the same as the samples used for mass gain (50 × 25 × 1.2 mm). However, when processing at 2.5 kHz, a different geometry shunt sample was required, in order to maintain a constant current through the monitoring sample. These samples were 120 × 10 × 1.2 mm, so that they had the same width as the monitoring sample. This was required so that the high local electrical field at the sample edges would be similar in both samples, keeping the current at a more consistent value.

A funnel was placed over the monitoring sample, with a hole in the side to allow the rod making the electrical connection to pass through. The funnel was sealed to the rod, to prevent gas escape, using a silicone gasket, which was attached to the rod and pushed up against the funnel. A measuring cylinder filled with electrolyte was placed over the funnel, so that gas evolved by the monitoring sample would be collected in the cylinder. The counter-electrode was a stainless steel ring lowered into the tank, but kept above the bottom of the funnel to avoid gas being collected from the counter-electrode. The shunt sample was also positioned above the bottom of the measuring cylinder to prevent unwanted gas collection. This arrangement is depicted in Fig.1.

It was decided that, while conventional sectioning and study of (SEM) micrographs are commonly used to monitor the progression of coating formation, a more reliable and accurate technique was required for the present study. This was done via sample weighing, using a balance with a resolution of about ±1 mg (and samples masses were

around four grams). Different samples (with the same dimensions) were processed for a range of times, spaced 3 minutes apart, and the mass gain measured in each case after careful washing and thorough drying. Of course, it should be possible to correlate the two types of measurement, although this does require knowledge of the porosity levels in the coatings. These are known [34] to be relatively high (typically of the order of 15-20%) in PEO coatings, but also to vary significantly and to be difficult to measure accurately, so such correlation is not straightforward. The weighing method is certainly considered to be more reliable and accurate: clearly, it reflects the average rate of oxide formation over the surface of the sample.

3 Synchronised Current and Video Monitoring

3.1 Global and Local Current and Voltage Characteristics at 50 Hz

Fig.2(a) shows a typical voltage profile during a single 50 Hz cycle (ie over a period of 20 ms), at a stage when the coating thickness was about 50 μm. This voltage acts across both large and small area samples. It can be seen that the profile approximates to a square wave, with the anodic voltage being ~600 V, while the cathodic voltage is ~125 V. It should be noted that these voltages are not pre-selected, but are adjusted by the machine to maintain the set current values. Fig.2(b) shows corresponding currents, both the total and that through the small area sample. Apart from short initial transients, the total current was just above 2 A throughout both anodic and cathodic half-cycles (corresponding, at least approximately, to the pre-selected current density of 30 A dm^{-2}).

It can be seen that the cathodic current through the small area reflects the total current, taking account of the area ratio between small and large samples. (It may be noted that current densities are in general not exactly the same for the two, since edge effects lead to a more divergent electric field for the small area sample and some coating tends to form on the cylindrical face between the wire and the resin. The upshot of this is that the current density on the small area sample is likely to be greater by a relatively small factor, of the order of 3-5.) The plots in Fig.2(b) suggests a cathodic process that is smooth and continuous, such as might be expected for conversion of protons to hydrogen gas. In contrast to this, the anodic current is made up of a series of current pulses corresponding to discharges. The integrated area of these pulses in a single half-cycle does not necessarily correspond to the area-normalised total current, since there are likely to be variations in the number of discharges in each cycle and, indeed, there may be periods of several cycles when there are no discharges in the small sample. Fig.3 shows nine images of the small area sample, taken at different times during the anodic part of the cycle shown in Fig. 2. It can be seen that the periods during which there are current pulses correspond with images in which light is being emitted from two distinct points on the surface of the sample, corresponding to two active discharge cascades. Observations of this type, which have been reported previously in some detail [7, 8, 35], confirm that the anodic current pulses arise from cascades of discharges, which tend to occur in particular locations. These characteristics, including the absence of well-defined

discharges in the cathodic half-cycle, are consistent with the majority of previous observations and reports.

3.2 The Effect of Supply Frequency on Discharge Characteristics

As the supply frequency was increased, and the half-cycle period started to approach typical lifetimes of the discharges, certain changes were observed in the nature of the voltage and current profiles, although, as with the behaviour at 50 Hz, there were some cycles in which no discharges occurred on the small sample. Fig.4, which shows electrical profiles from experiments carried out at 2.5 kHz after 18 minutes of PEO processing, illustrates these changes. The voltage profiles (Fig.4(a)) are similar to those at 50 Hz (Fig.2(a)), except that the cathodic voltage has risen to about 250 V, compared to 125 V at 50 Hz, while the anodic voltage remained unchanged at about 600 V. This suggests a switch to a cathodic process that requires a larger driving force. It is also clear from the current profiles (Fig.4(b)) for the small area that changes have occurred in phenomena occurring during the cathodic part of the cycle. While the anodic discharges are still taking place with approximately unchanged lifetimes, of the order of 100–200 μs (now occupying most of the half-cycle), and similar current levels of ~50–100 mA, there are now clear current pulses in the cathodic part of the cycle as well. Moreover, some of these pulses rise to higher current levels than those of the anodic discharges, with peaks approaching 200 mA. Other experimental runs were carried out over a range of processing frequencies. Cathodic discharges were only detected above a supply frequency of 1.75 kHz.

Confirmation that these cathodic pulses correspond to discharges is provided by high speed photography observations. The images in Fig.5 show superimpositions of the set of frames (25 images) covering each half-cycle. It can be seen that light emission accompanies both anodic and cathodic pulses. It also appears that, as for the anodic discharges, those in the cathodic half-cycle also occur in spatially localised cascades. In the example shown in Fig.5, the two types of discharge occur in different locations, although this is not necessarily a general feature, and they have also been observed to occur in the same location.

4 Promotion of Cathodic Discharges

4.1 Effect of Coating Thickness

No cathodic discharges were recorded during 50 Hz processing of Al in this work, which is consistent with previous reports. However, as shown above, cathodic discharges can occur when processing with high (2.5 kHz) frequency. The effects of coating thickness were investigated using Al-1050 plates, processed for various times. Mass gain and thickness measurements are presented in Fig.6. It can be seen that a change occurred after about 25 minutes, when the rate of coating growth dropped significantly. (This can be seen more clearly in the weight gain data, which are more accurate and reliable than thickness changes measured via metallographic sectioning.)

It became clear that this transition (during processing at high frequency) coincided, at least approximately, with the onset of cathodic discharge formation. These started to

form only after the coating thickness had reached about 30–40 μm. Fig.7 shows the number of cathodic and anodic discharges observed during periods of 173 ms (covering ~430 voltage cycles), on a 30 mm^2 area in the centre of the plates, after different processing times. The number of active discharge sites in this area, at any given time, is relatively small, so there are some statistical fluctuations in these data. Nevertheless, a clear trend is apparent, with cathodic discharges starting to occur after ~20 minutes of processing, when the coating was ~35 μm thick, and rising to a plateau value afterwards. Anodic discharges, on the other hand, occurred throughout the process, with their frequency dropping off somewhat with increasing time. (This kind of effect - ie anodic discharges becoming rather less frequent, but more energetic, as the coating becomes thicker, has been observed many times previously.) Noting the log scale of this plot, it can be seen that, even when cathodic discharges become established, they remain substantially less common than anodic ones.

The evolution of the applied potential during processing, which automatically adjusted to achieve the set current density of 30 A dm^{-2}, is shown in Fig.8. The anodic voltage for both high and low frequency remained very similar throughout processing. The cathodic voltage, at 50 Hz, gradually increased with processing time, from around -110 V to -145 V after 30 minutes of processing. At 2.5 kHz, the cathodic voltage increased more significantly, rising from -135 V to -250 V in the first 20 minutes of processing, and then at a more gradual rate for the remaining 10 minutes. This implies that the current-carrying process during cathodic polarisation is more difficult at higher frequencies, particularly as the coating becomes thicker. In fact, it's clear that the onset of cathodic discharges coincides with the cathodic voltage reaching a level sufficient to stimulate dielectric breakdown across the residual oxide layer on the substrate. It also seems clear that this current-carrying process must be flow of protons through the column of electrolyte in the pore above this layer (followed by them being discharged and released as hydrogen gas when they reach it). This process clearly becomes slower as the coating thickness increases, and is probably also somewhat inhibited by high pH and by a high supply frequency.

4.2 Microstructural Effects

Plates processed for 3, 12 and 30 minutes, at 50 Hz and 2.5 kHz, were examined microstructurally. Two samples (25 × 12.5 mm) were cut from each plate. One was used to examine the free surface in the SEM, and the other was mounted, ground and polished to view the cross-section.

The micrographs in Fig.9 and 10 show coating free surfaces and typical sections, at 50 Hz and 2.5 kHz, respectively after 3 minutes and 12 minutes. In general, samples processed for the same times at the two frequencies had similar microstructures. At short processing times, the discharge channel pores are relatively small (a few μm diameter) and numerous. Longer processing causes the features to coarsen, with pancake diameters reaching a few tens of microns across, as has been widely reported. However, the sample processed for 30 minutes at 2.5 kHz was observed to contain large,

deep craters, of the type visible in Fig.11, which were not present in the 30 minute sample processed at 50 Hz. These craters are large (up to 100 µm across) and deep.

It seems likely that these craters were the result of cathodic discharges, quite possibly as a consequence of energetic, long-lived cascades. It is certainly clear that they form only under the conditions (high frequency, with relatively thick coatings) confirmed above as being those that are required in order to stimulate such discharges.

5 Effects of Cathodic Discharges

5.1 Gas Evolution Rates

As outlined in §2.3, only net gas evolution rates were measured, with no compositional analysis. The results are shown in Fig.12, together with the mass gain of standard plate samples processed under similar conditions - ie the data presented in Fig.6. It can be seen that the gas evolution rate and mass gain rate are approximately constant throughout processing at 50 Hz supply frequency. However, with a 2.5 kHz supply frequency, the gas evolution rate follows the same trend as 50 Hz up until ~20 minutes of processing, when there is a significant increase in the gradient. This coincides with the change in the rate of mass gain. As noted above, this levels off completely after ~25 minutes of processing. It can be seen that all of the gas evolution rates are significantly higher than the maximum electrochemical Faraday gas yield, which is based on all of the current (~0.6 A) producing H_2 under cathodic polarisation, and O_2 under anodic polarization.

As noted in the Introduction, gas liberation rates during PEO have repeatedly been observed to exceed the Faraday yield. It may be helpful at this point to highlight some simple calculations that can be made concerning gas evolution. For 50 Hz, with no cathodic discharges, all of the cathodic current is carried by hydrogen evolution on the sample. Assuming that this hydrogen is an ideal gas, the volume produced is

$$v_c = \frac{nRT}{P} \tag{1}$$

where R is the gas constant, T is the absolute temperature, P is the pressure and n is the number of moles of gas. This may be written as

$$n = \frac{I_c t}{4F} \tag{2}$$

where I_c is the average cathodic current through the sample, t is the processing time and F is the Faraday constant. The factor of 4 comes from the cathodic half-cycle being 50% of the time, and one mole of e^- forms ½ mole of H_2 gas. It follows that

$$v_c = \frac{I_c tRT}{4FP} \tag{3}$$

During the 50 Hz run concerned, I_c = 0.82 A, and the temperature was ~22˚C (295 K). This leads, for a time of 30 minutes, to v_c ~90 mL, assuming the pressure to be atmospheric (1 bar).

To produce the oxygen present in the coating, water must be decomposed, causing hydrogen gas to be released. Assuming that the coating is pure alumina, the volume of hydrogen gas evolved in this way at the anode, v_a, is given by a corresponding set of equations

$$v_a = \frac{nRT}{P} \tag{4}$$

with the number of moles now given by

$$n = \frac{\Delta m}{M_{r(O)}} \tag{5}$$

where Δm is the mass gain of the monitoring sample and $M_{r(O)}$ is the molecular weight of oxygen. The volume of gas produced in this way (during the anodic half-cycle) is thus

$$v_a = \frac{\Delta mRT}{M_{r(O)}P} \tag{6}$$

For the 50 Hz case, after 30 minutes, Δm = 0.0126 g, giving v_a = 19 mL. The observed amount of gas evolved during this run was v_{total} = 320 mL, so that this was only a relatively small contribution.

The remainder of the gas evolved, which was about 210 mL (ie about 65% of the total), must have been produced via thermal decomposition of water molecules. Relatively large quantities of water certainly enter the plasma and become ionized during discharge formation. It is thermodynamically favourable for them all (apart from the small amount of oxygen used to form the metal oxide, accounted for above) to combine and reform H_2O when the plasma cools and collapses. However, it must be recognized that this cooling occurs in the form of a dramatic quench and it would certainly not be surprising if the kinetics were such that this process remained incomplete, leading to the release of relatively large amounts of gas in the form of H_2 and O_2 molecules.

The observed increase in rate of gas evolution for 2.5 kHz processing occurred at about the same time as the cathodic discharges started to take place. It seems highly likely that these were responsible for the increased gas evolution rate. This is, of course, expected, since the same mechanism - ie water entering the plasma, being ionized and these ions failing to fully recombine on cooling - is also expected to operate when the discharges are cathodic. Of course, this is a completely different mechanism from the simple electro-chemical basis of the Faraday yield calculation. There is no obvious upper bound that can be placed on the quantity of gas produced in this way, since the electrical input power during PEO is large compared to the energy required to produce this volume of gas by thermal decomposition of H_2O molecules [8]. It follows that, with discharges occurring during both half-cycles, the gas evolution rate should increase significantly, and, in fact, it almost doubles after cathodic discharges start to occur.

5.2 Coating Formation Rates

Also requiring explanation is the observed sharp drop in the rate of mass gain (ie the oxide formation rate) as cathodic discharges become common. At first glance, this looks rather surprising, since it might have been expected to rise (with oxide now being formed, via similar mechanisms, in both anodic and cathodic parts of the cycle). However, the observations made regarding the nature of the cathodic discharges are likely to be relevant here. There are certainly indications, such as the relatively high discharge currents in Fig.4, that cathodic discharges tend to be more energetic than anodic ones. This is consistent with the microstructural observations, with cathodic discharge sites, such as those in Fig.11, showing evidence of more violent events than those typical of anodic discharges. It certainly seems possible that, rather than new (molten) oxide being redistributed fairly smoothly around adjoining regions of the coating, as apparently happens during anodic discharges, cathodic discharges may result in much of this material (possibly plus previously-formed oxide in the vicinity) being ejected into the electrolyte. This could, of course, give rise to almost any net rate of mass change, including the observed one of being close to zero.

It may also be noted that losing material in this way during individual discharges in a cascade sequence might be expected to prolong that cascade. New oxide formation normally leads eventually to the electrical resistance of the region rising sufficiently to terminate the cascade, but this mechanism would not operate effectively under these circumstances. This is something that it should be possible to confirm experimentally, although tracking an individual cascade through its complete lifetime is not simple, using either electrical or optical monitoring, because these cascade lifetimes tend in any event to be very long on the scale of discharge lifetimes.

6 Conclusions

The information presented here from synchronised high speed video and electrical monitoring, as well as microstructural observations and gas monitoring, allow the following conclusions to be drawn:

(a) High frequency processing leads to initiation of discharges during the cathodic half-cycle, but only after a certain coating thickness has been reached. This was ~30-40 μm for the present conditions. This was confirmed by electrical monitoring, which showed distinct current pulses on a small area sample during the cathodic half-cycle, and also by high speed photography, showing light emission accompanying these current pulses.

(b) Cathodic discharges occur when the cathodic voltage rises sufficiently. These experiments were carried out under constant current conditions, such that the voltage rises if and when the corresponding current starts to fall. This occurred only with a high frequency supply and when the coating had become relatively thick. It seems likely that this represented a condition such that the required current could not be sustained solely by flow of protons through electrolyte channels above the thin oxide layer through which electron flow occurs. Once the applied voltage reached a sufficiently high level (~250 V in the present work), cathodic discharges started to occur. These carry the imposed current without the requirement extensive proton flow through long electrolyte channels.

(c) Cathodic discharges occur in cascades at particular spatial locations. They tend to reach higher peak currents, dissipate more electrical energy and emit light more intensely than typical anodic discharges.

(d) Mass gain and coating thickness tend to increase linearly for low frequency processing. However, rates of both mass gain and coating thickness increase tend to fall off to low levels during high frequency processing, after the initiation of cathodic discharges.

(e) It is suggested that the reduced rate of coating formation after the onset of cathodic discharges is related to their highly energetic nature, possibly causing loss of coating material to the electrolyte via the ejection of recently-formed and/or previously-formed oxide. The sites of recent cathodic discharge cascades exhibited large craters suggestive of this.

(f) Measured rates of gas evolution during processing were well above Faraday yield (purely electro-chemical) levels. This is thought to be a consequence of discharge formation, with water entering the plasma and breaking down into various ionised species. Recombination to form water does occur as the plasma collapses and is quenched, but this is incomplete. Consistent with this picture, the rate of gas evolution goes up significantly after the onset of cathodic discharge formation.

Acknowledgements

This work has been supported by EPSRC (grant number EP/I001174/1), by a Sims Scholarship (for SCT) in Cambridge University and by Keronite plc. The latter collaboration has included extensive interactions with Keronite personnel, including Robin Francis and Mike Coto. Thanks are also due to Jamie Bragg, of Cambridge University, who carried out some of the experimental work and took part in useful discussions.

In compliance with EPSRC requirements, raw data in the form of selected video and discharge current files are available at www.ccg.msm.cam.ac.uk/publications/resources, and are also accessible via the University repository at http://www.data.cam.ac.uk/repository.

References

[1] Dunleavy CS, Golosnoy IO, Curran JA, Clyne TW. Characterisation of discharge events during plasma electrolytic oxidation. Surface and Coatings Technology. 2009;203:3410–9.
[2] Kasalica B, Petkovic M, Belca I, Stojadinovic S, Zekovic L. Electronic transitions during plasma electrolytic oxidation of aluminum. Surf Coat Technol. 2009;203:3000-4.
[3] Martin J, Melhem A, Shchedrina I, Duchanoy T, Nomine A, Henrion G, et al. Effects of electrical parameters on plasma electrolytic oxidation of aluminium. Surf Coat Techn. 2013;221:70-6.
[4] Hussein RO, Nie X, Northwood DO. A spectroscopic and microstructural study of oxide coatings produced on a Ti–6Al–4V alloy by plasma electrolytic oxidation. Materials Chemistry and Physics. 2012;134:484-92.
[5] Dunleavy CS, Curran JA, Clyne TW. Self-similar scaling of discharge events through PEO coatings on aluminium. Surface and Coatings Technology. 2011;206:1051-61.
[6] Dunleavy CS, Curran JA, Clyne TW. Time dependent statistics of plasma discharge parameters during bulk AC plasma electrolytic oxidation of aluminium. Applied Surface Science. 2013;268:397-409.
[7] Nomine A, Troughton SC, Nomine AV, Henrion G, Clyne TW. High speed video evidence for localised discharge cascades during plasma electrolytic oxidation. Surf Coat Technol. 2015; 269:125–30.
[8] Clyne TW, Troughton SC. A review of recent work on discharge characteristics during plasma electrolytic oxidation of various metals. International Materials Reviews. 2018;63:1-36.
[9] Matykina E, Arrabal R, Pardo A, Mohedano M, Mingo B, Rodriguez I, et al. Energy-efficient PEO process of aluminium alloys. Materials Letters. 2014;127:13-6.
[10] Troughton SC, Nomine A, Nomine AV, Henrion G, Clyne TW. Synchronised Electrical Monitoring and High Speed Video of Bubble Growth associated with Individual Discharges During Plasma Electrolytic Oxidation. Applied Surface Science. 2015;359:405-11.
[11] Zhang XM, Tian XB, Yang SQ, Gong CZ, Fu RKY, Chu PK. Low energy-consumption plasma electrolytic oxidation based on grid cathode. Review of Scientific Instruments. 2010;81. 103504.
[12] Zhang XM, Tian XB, Gong CZ, Yang SQ. Discharge characteristics of confined cathode micro-arc oxidation. Acta Physica Sinica. 2010;59:5613-9.
[13] Xin SG, Song LX, Zhao RG, Hu XF. Influence of cathodic current on composition, structure and properties of Al2O3 coatings on aluminum alloy prepared by micro-arc oxidation process. Thin Solid Films. 2006;515:326-32.
[14] Li QB, Liang J, Liu BX, Peng ZJ, Wang Q. Effects of cathodic voltages on structure and wear resistance of plasma electrolytic oxidation coatings formed on aluminium alloy. Applied Surface Science. 2014;297:176-81.
[15] Wang JH, Du MH, Han FZ, Yang J. Effects of the ratio of anodic and cathodic currents on the characteristics of micro-arc oxidation ceramic coatings on Al alloys. Applied Surface Science. 2014;292:658-64.
[16] Rakoch AG, Gladkova AA, Linn Z, Strekalina DM. The evidence of cathodic micro-discharges during plasma electrolytic oxidation of light metallic alloys and micro-discharge intensity depending on pH of the electrolyte. Surf Coat Technol. 2015;269:138-44.
[17] Sah SP, Tsuji E, Aoki Y, Habazaki H. Cathodic pulse breakdown of anodic films on aluminium in alkaline silicate electrolyte - Understanding the role of cathodic half-cycle in AC plasma electrolytic oxidation. Corrosion Science. 2012;55:90-6.
[18] Nomine A, Martin J, Noel C, Henrion G, Belmonte T, Bardin IV, et al. The evidence of cathodic micro-discharges during plasma electrolytic oxidation process. Appl Phys Lett. 2014;104:Art. 081603.
[19] Nomine A, Martin J, Henrion G, Belmonte T. Effect of cathodic micro-discharges on oxide growth during plasma electrolytic oxidation (PEO). Surf Coat Technol. 2015;269:131-7.
[20] Nominé A, Nominé AV, Braithwaite NS, Belmonte T, Henrion G. High-frequency induced Cathodic Breakdown during Plasma Electrolytic Oxidation. Appl Phys Lett. 2017;submitted.
[21] Stojadinovic S, Tadic N, Sisovic NM, Vasilic R. Real-time imaging, spectroscopy, and structural investigation of cathodic plasma electrolytic oxidation of molybdenum. Journal of Applied Physics. 2015;117. 233304.
[22] Snizhko LO, Yerokhin AL, Pilkington A, Gurevina NL, Misnyankin DO, Leyland A, et al. Anodic processes in plasma electrolytic oxidation of aluminium in alkaline solutions. Electrochimica Acta. 2004;49:2085–95.

[23] Snizhko LO, Yerokhin AL, Gurevina NL, Patalakha VA, Matthews A. Excessive Oxygen Evolution during Plasma Electrolytic Oxidation of Aluminium. Thin Solid Films. 2007;516:460-4.
[24] Snezhko LA, Erokhin AL, Kalinichenko OA, Misnyankin DA. HYDROGEN RELEASE ON THE ANODE IN THE COURSE OF PLASMA ELECTROLYTIC OXIDATION OF ALUMINUM. Materials Science. 2016;52:421-30.
[25] Cheng YL, Peng ZM, Wua XQ, Cao JH, Skeldon P, Thompson GE. A comparison of plasma electrolytic oxidation of Ti-6Al-4V and Zircaloy-2 alloys in a silicate-hexametaphosphate electrolyte. Electrochimica Acta. 2015;165:301-13.
[26] Cheng YL, Wang T, Li SX, Cheng YL, Cao JH, Xie HJ. The effects of anion deposition and negative pulse on the behaviours of plasma electrolytic oxidation (PEO)-A systematic study of the PEO of a Zirlo alloy in aluminate electrolytes. Electrochimica Acta. 2017;225:47-68.
[27] Sengupta SK, Srivastava AK, Singh R. Contact glow discharge electrolysis: A study on its origin in the light of the theory of hydrodynamic instabilities in local solvent vaporisation by Joule heating during electrolysis. Journal of Electroanalytical Chemistry. 1997;427:23-7.
[28] Sengupta SK, Singh R, Srivastava AK. A study on the origin of nonfaradaic behavior of anodic contact glow discharge electrolysis - The relationship between power dissipated in glow discharges and nonfaradaic yields. Journal of the Electrochemical Society. 1998;145:2209-13.
[29] Yao ZP, Xu YJ, Jiang ZH, Wang FP. Effects of cathode pulse at low frequency on the structure and composition of plasma electrolytic oxidation ceramic coatings. Journal of Alloys and Compounds. 2009;488:273-8.
[30] Yao ZP, Liu YF, Xu YJ, Jiang ZH, Wang FP. Effects of cathode pulse at high frequency on structure and composition of Al2TiO5 ceramic coatings on Ti alloy by plasma electrolytic oxidation. Materials Chemistry and Physics. 2011;126:227-31.
[31] Wang HY, Zhu RF, Lu YP, Xiao GY, Ma J, Yuan YF. Preparation and Mechanism of Controllable Micropores on Bioceramic TiO2 Coatings by Plasma Electrolytic Oxidation. Surface Review and Letters. 2013;20. 1350051.
[32] Kharanagh VJ, Sani MAF, Rafizadeh E. Effect of current frequency on coating properties formed on aluminised steel by plasma electrolytic oxidation. Surface Engineering. 2014;30:224-8.
[33] Zou B, Lu GH, Zhang GL, Tian YY. Effect of current frequency on properties of coating formed by microarc oxidation on AZ91D magnesium alloy. Transactions of Nonferrous Metals Society of China. 2015;25:1500-5.
[34] Curran JA, Clyne TW. Porosity in plasma electrolytic oxide coatings. Acta Materialia. 2006;54:1985-93.
[35] Troughton SC, Nomine A, Dean J, Clyne TW. Effect of individual discharge cascades on the microstructure of plasma electrolytic oxidation coatings. Applied Surface Science. 2016;389:260-9.

Figure Captions

Fig.1 Schematic depiction of the gas collection system.

Fig.2 Experimental data obtained during a single cycle of PEO processing at 50 Hz, with a coating thickness of about 40 µm, showing: (a) voltage and (b) current (both total and that flowing through the small area sample).

Fig.3 High speed video images of the small area sample, taken during the run that produced the data in Fig.2. The times indicated correspond to the axes of those plots.

Fig.4 Experimental data obtained during a single cycle of PEO processing at 2.5 kHz, with a coating thickness of about 40 µm, showing: (a) voltage and (b) current (both total and that flowing through the small area sample).

Fig.5 High speed video images of the small area sample, taken during the run that produced the data in Fig.4, synchronized with the small area current plot.

Fig.6 Experimental data for weight gain and coating thickness, as a function of processing time, during PEO with two different supply frequencies.

Fig.7 Data for the areal and temporal frequency of both types of discharge during processing at 2.5 kHz, taken from a series of short video sequences (each ~0.17 s long), covering a representative (30 mm^2) area of the sample.

Fig.8 Evolution of the anodic and cathodic voltages during PEO processing at 50 Hz and 2.5 kHz.

Fig.9 Micrographs from samples processed for 3 minutes, showing (a) a free surface after processing at 50 Hz, (b) a free surface after processing at 2.5 kHz, (c) a transverse section after processing at 50 Hz and (d) a transverse section after processing at 2.5 kHz.

Fig.10 Micrographs from samples processed for 12 minutes, showing (a) a free surface after processing at 50 Hz, (b) a free surface after processing at 2.5 kHz, (c) a transverse section after processing at 50 Hz and (d) a transverse section after processing at 2.5 kHz.

Fig.11 Micrographs from a sample processed for 30 minutes at 2.5 kHz, showing (a) part of the free surface and (b) a transverse section through a large crater of the type visible in (a).

Fig.12 Experimental data for weight gain of standard plate samples (processed individually) and the volume of gas liberated from the monitoring sample, under similar conditions. Also shown is the maximum electrochemical Faraday yield line for gas evolution, with a monitoring sample current of 0.6 A.

Figure

Click here to download high resolution image

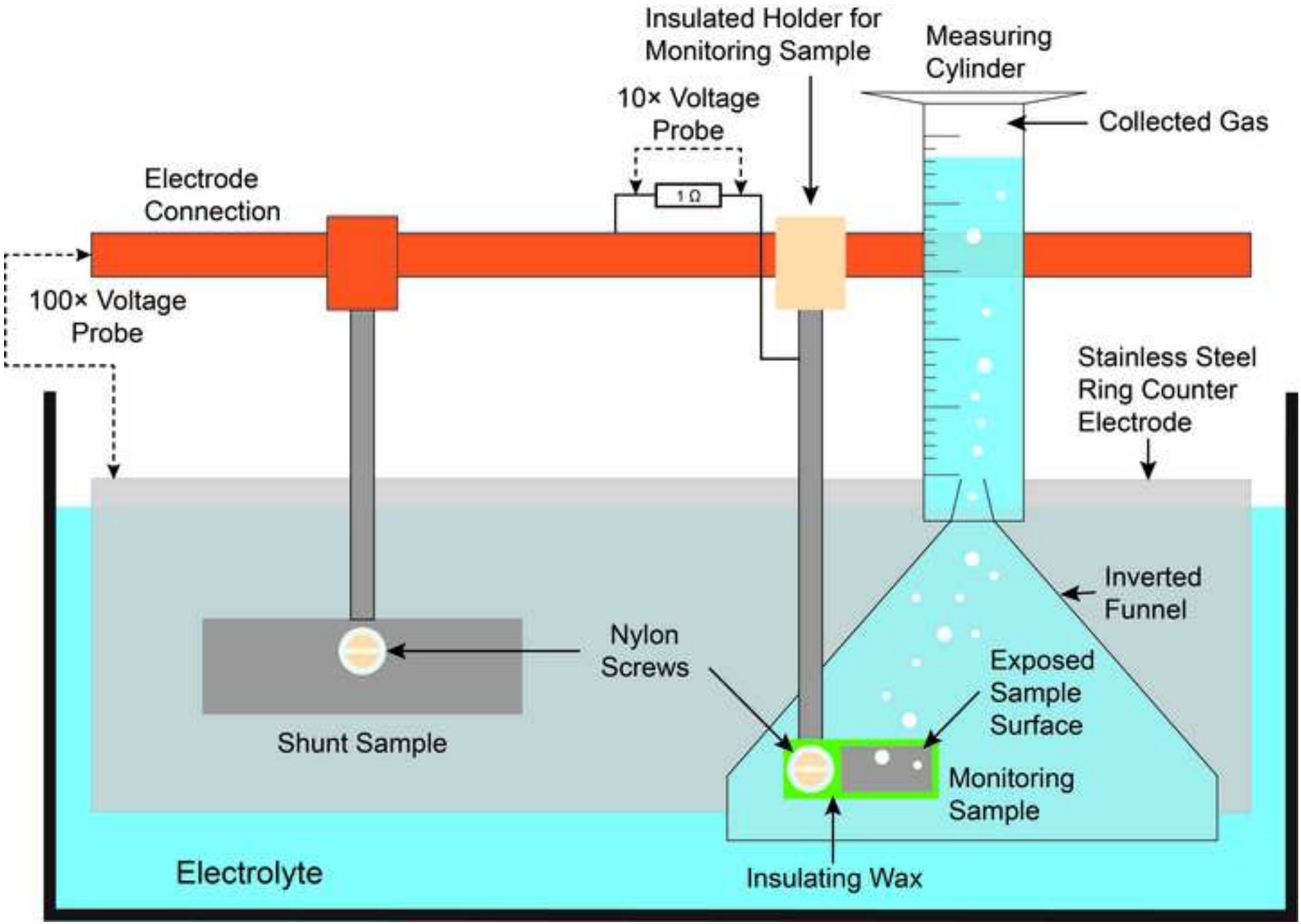

Figure

Click here to download high resolution image

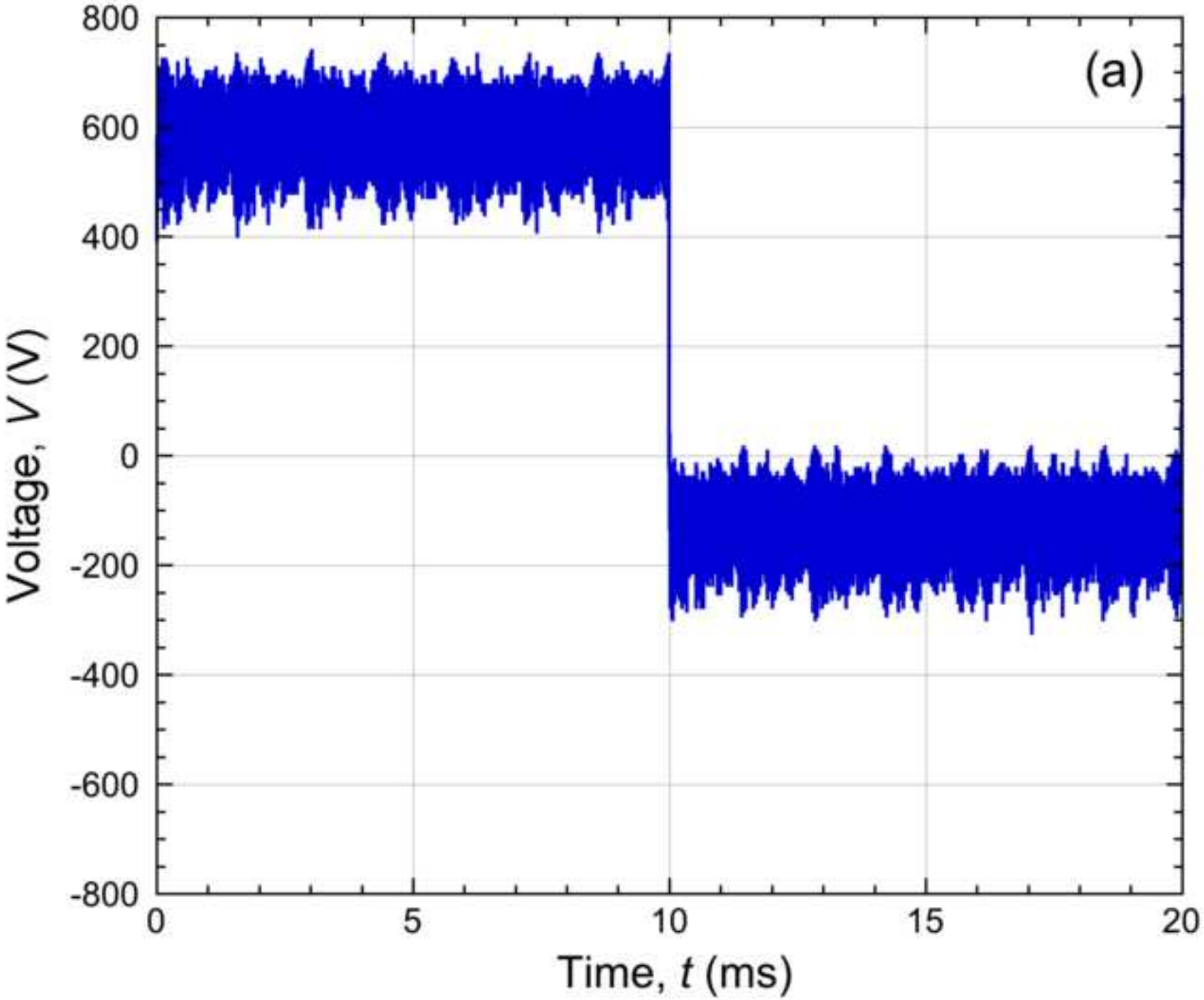

Figure
Click here to download high resolution image

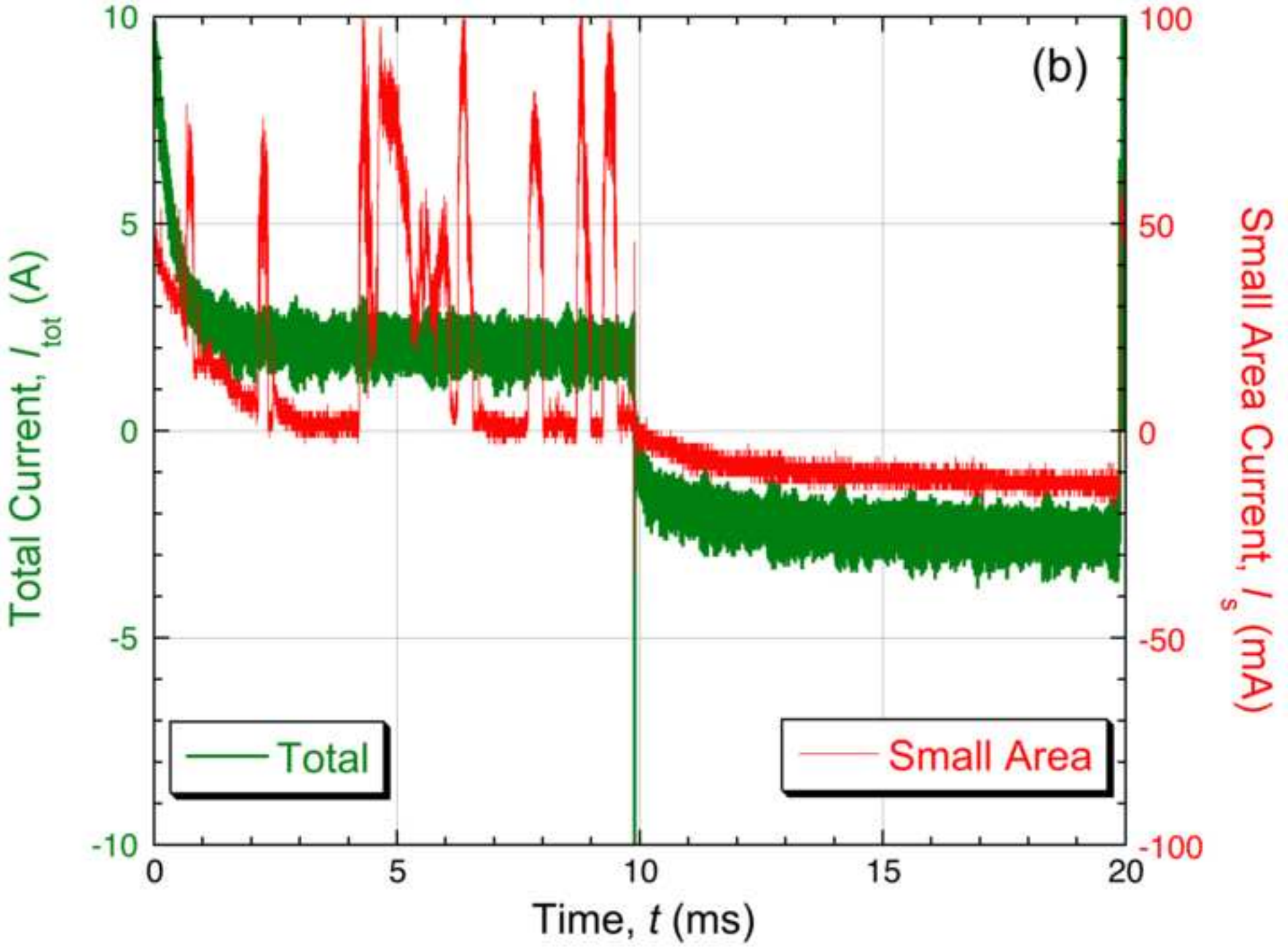

Figure

Click here to download high resolution image

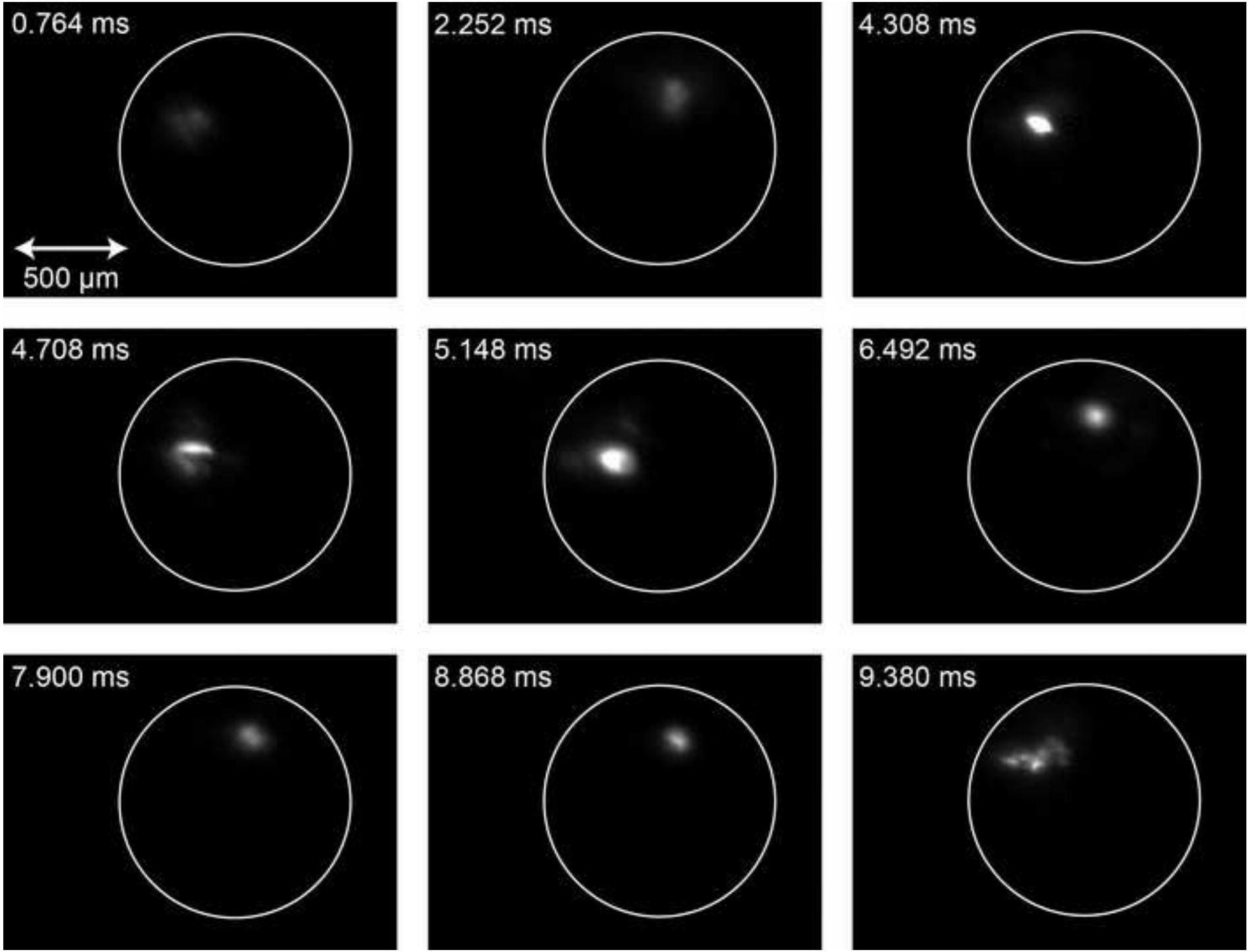

Figure

Click here to download high resolution image

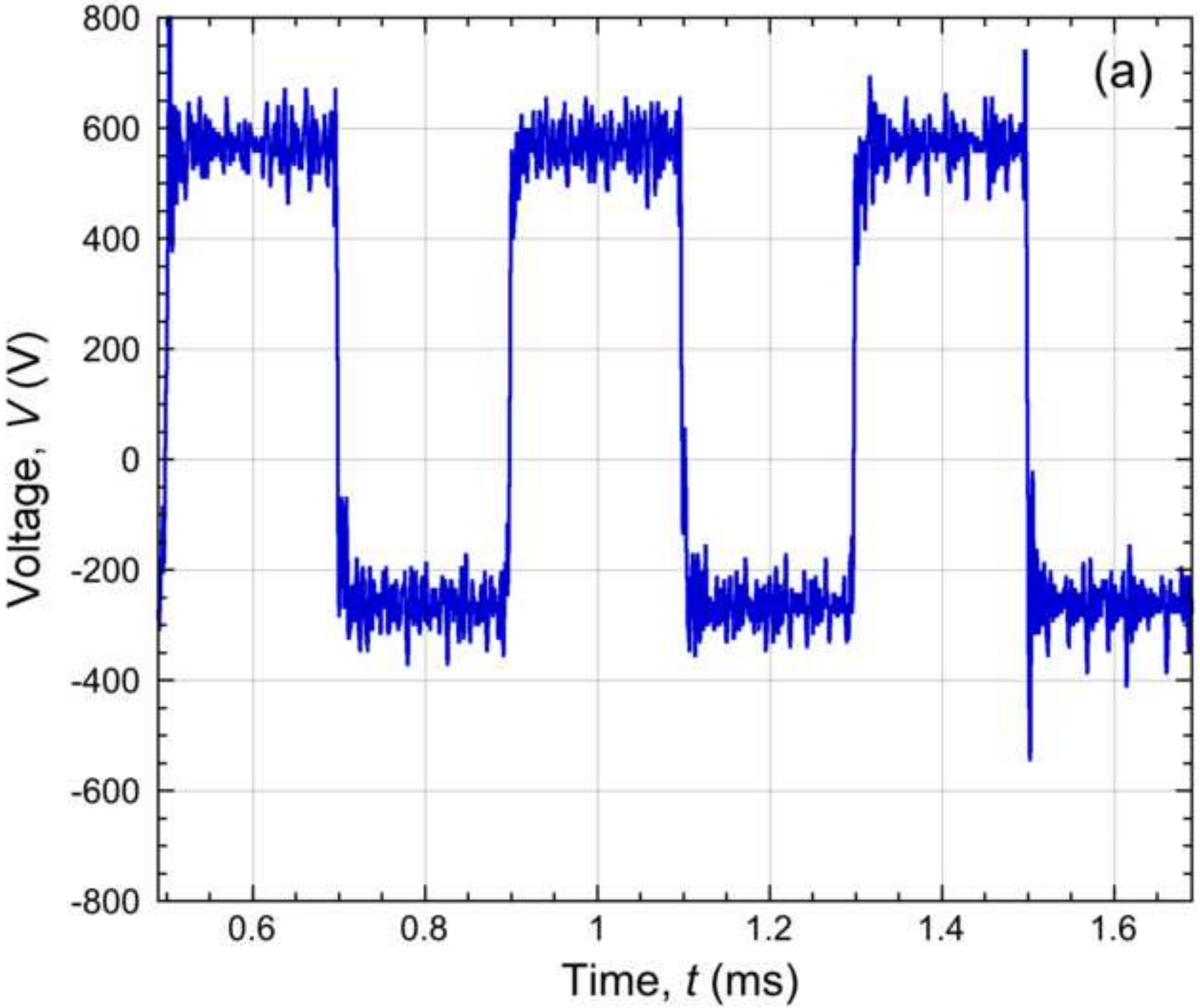

Figure

Click here to download high resolution image

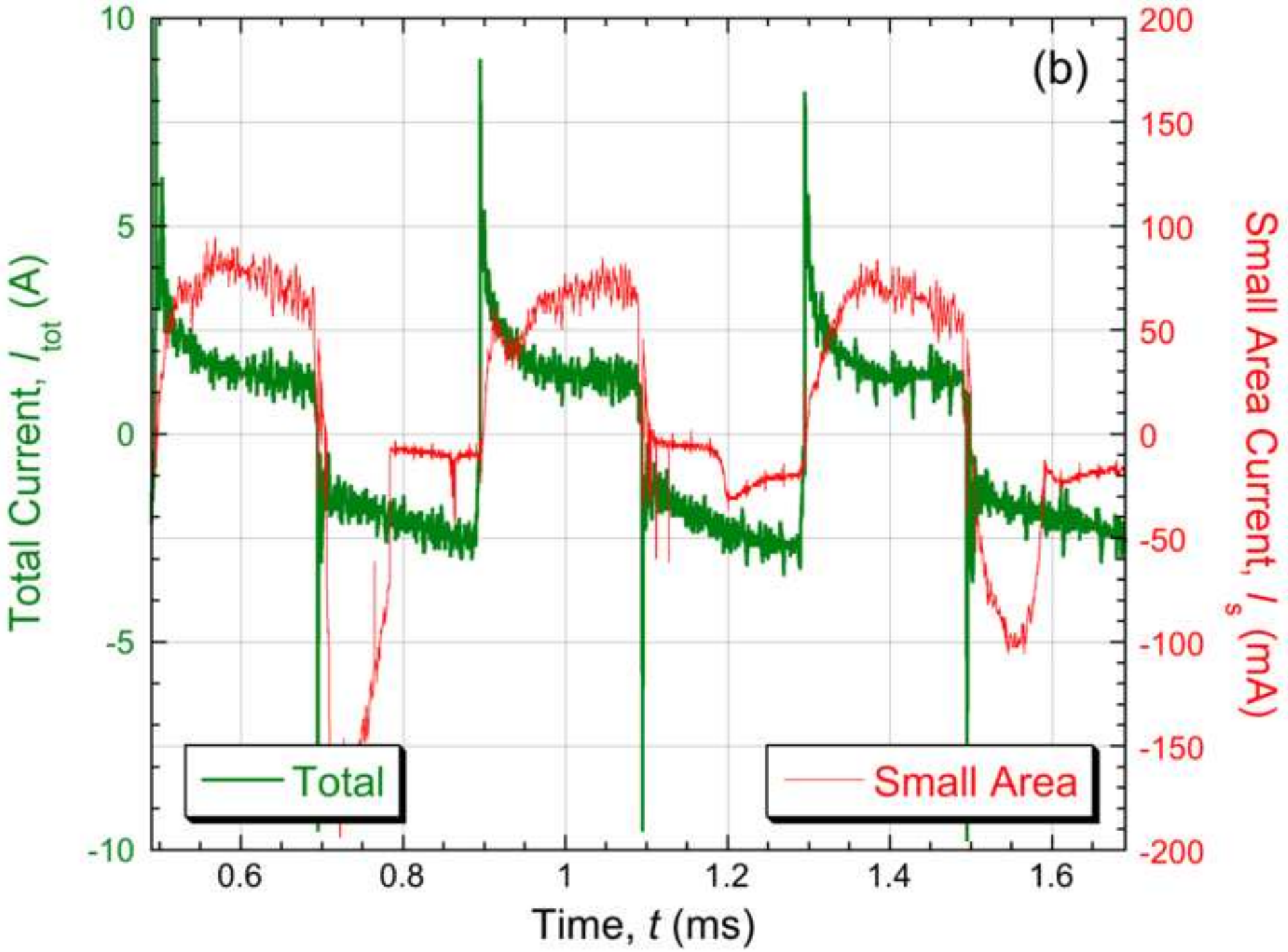

Figure

Click here to download high resolution image

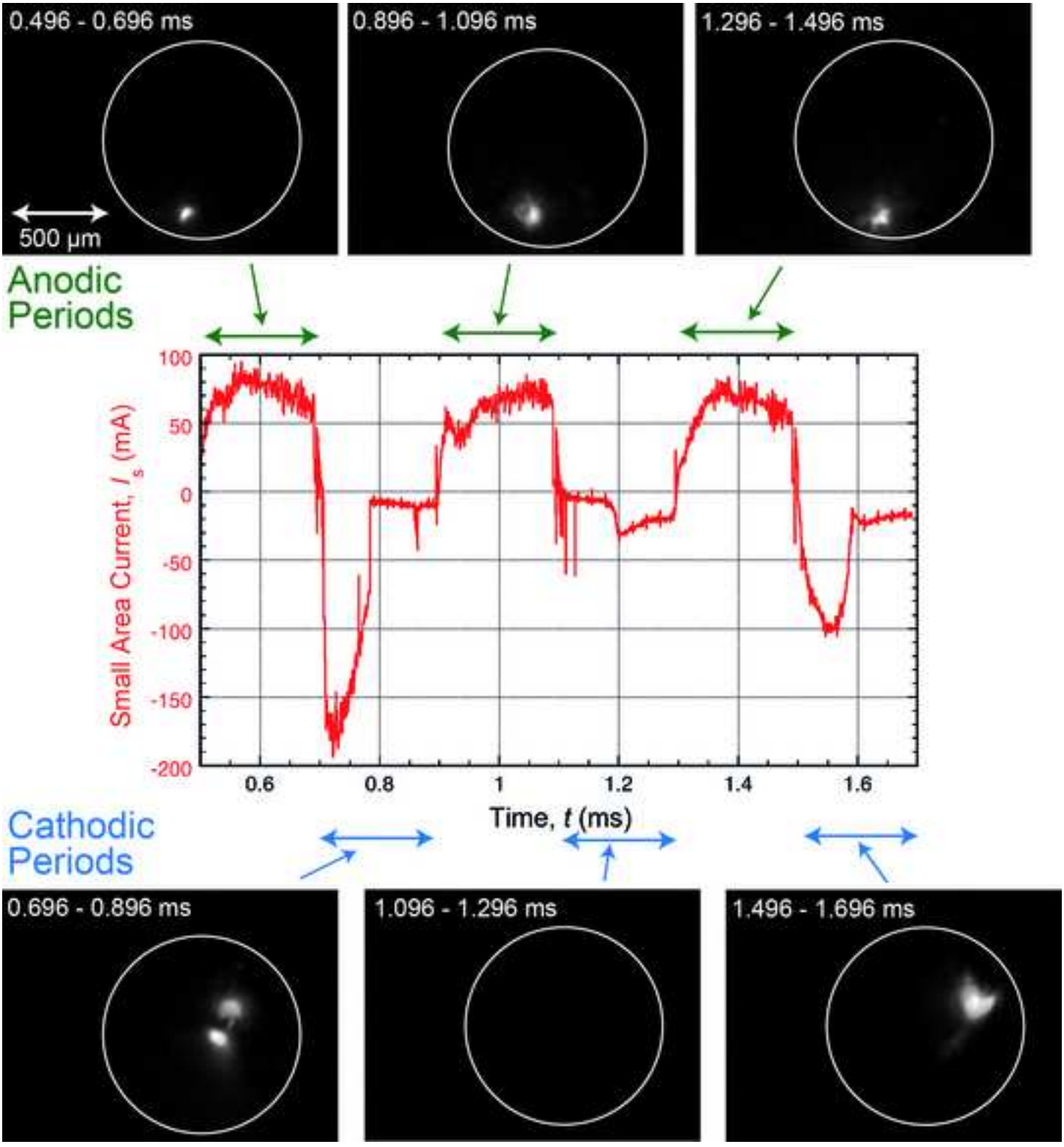

Figure
Click here to download high resolution image

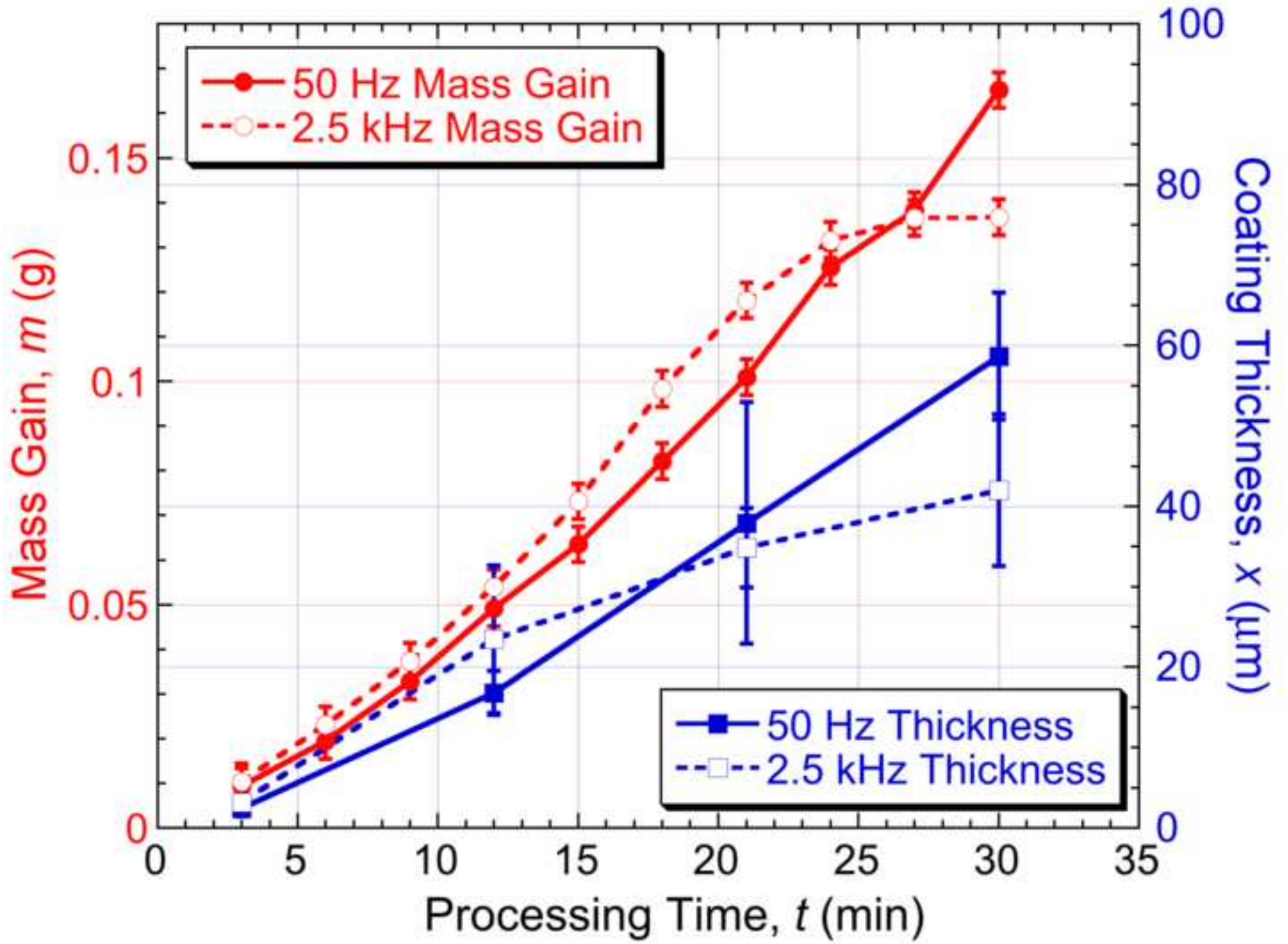

Figure

Click here to download high resolution image

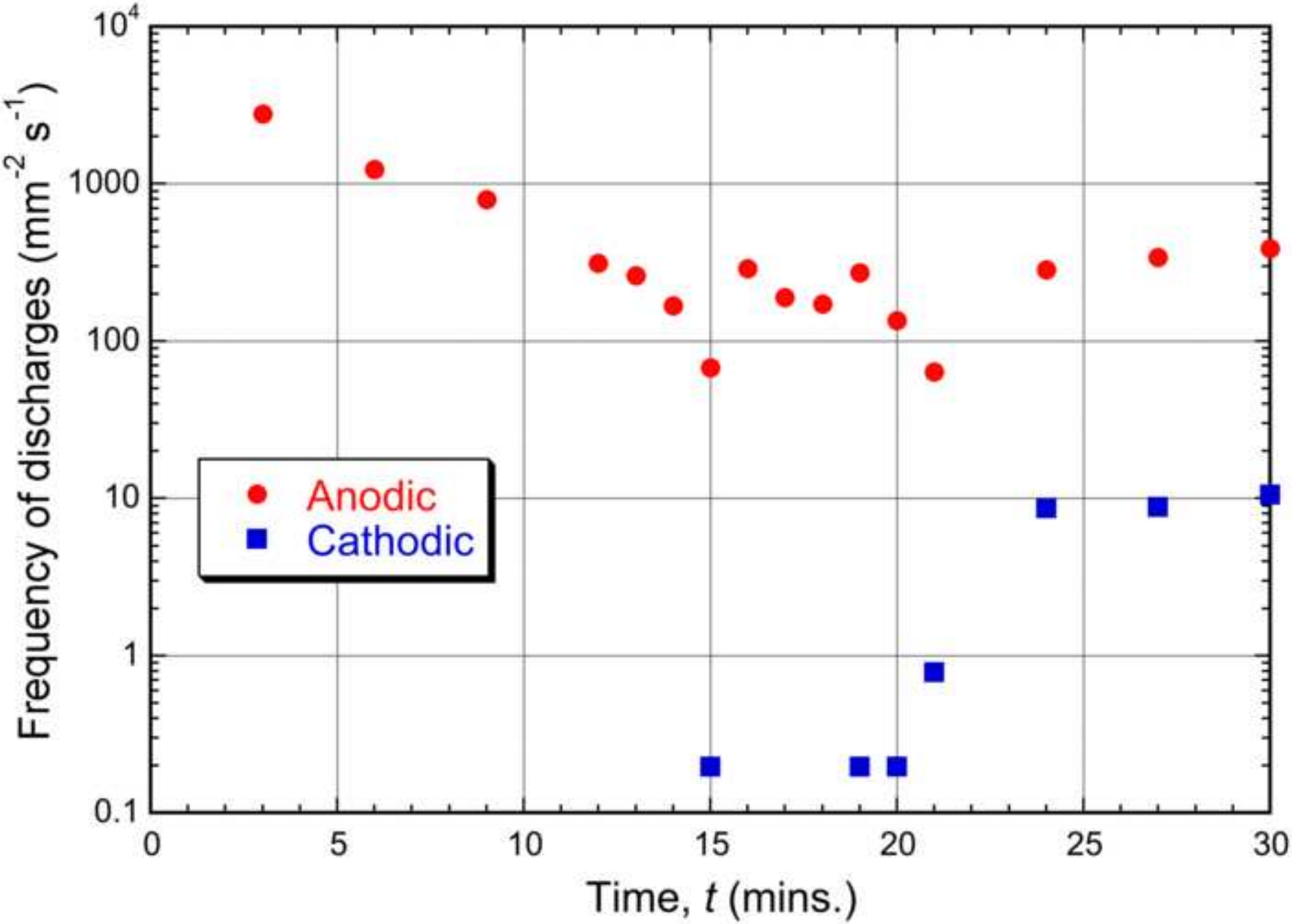

Figure

Click here to download high resolution image

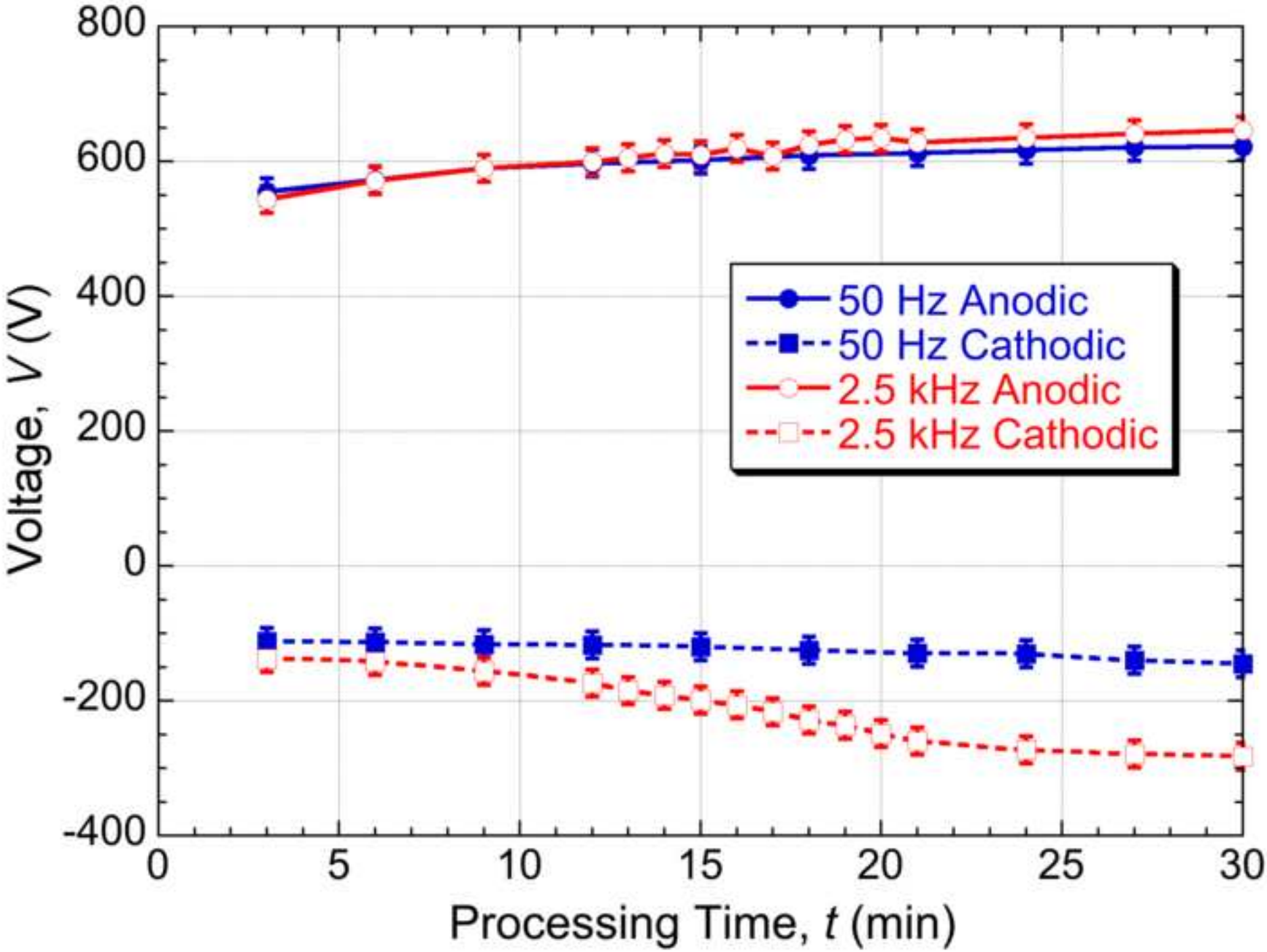

Figure

Click here to download high resolution image

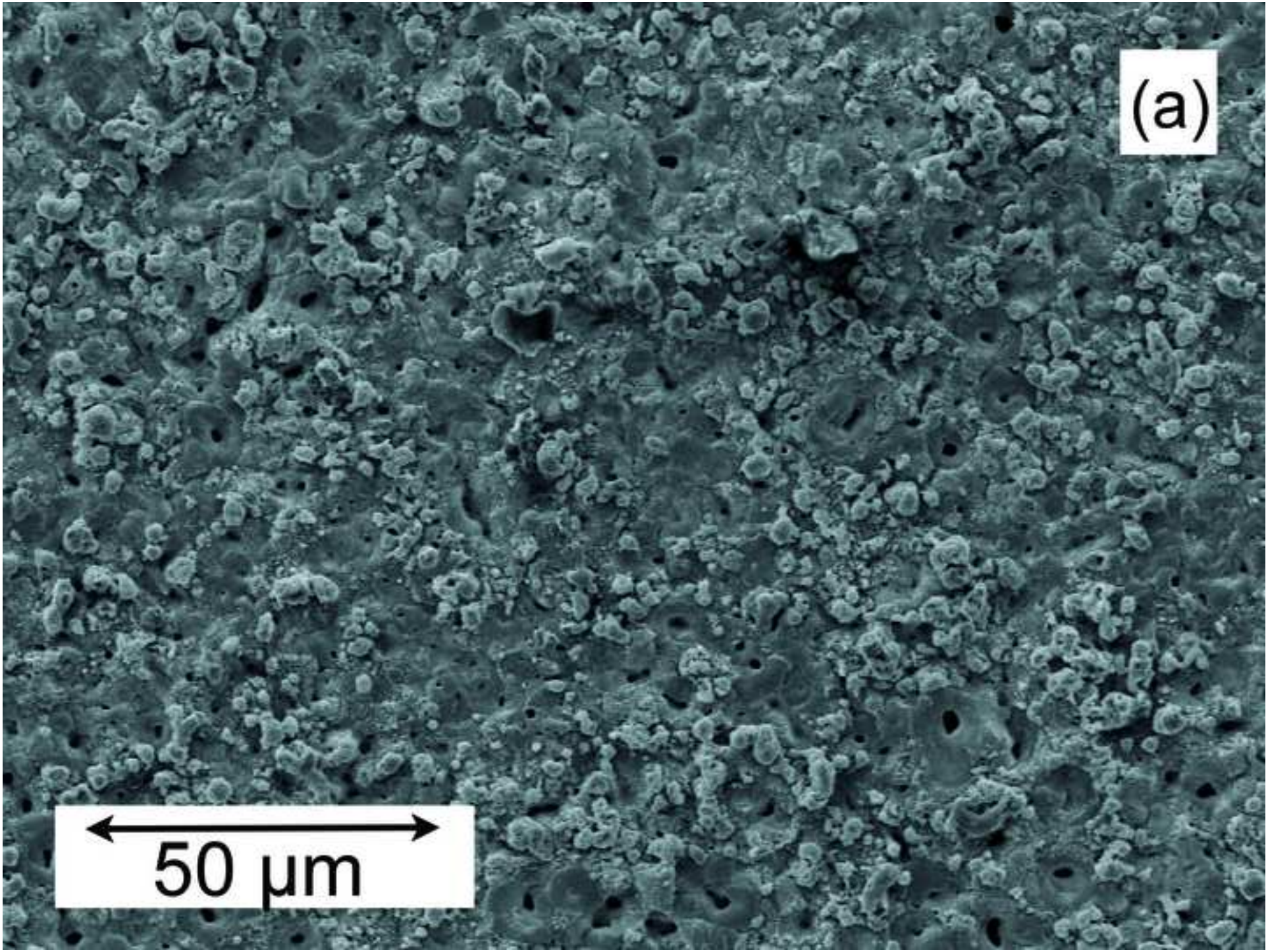

Figure

Click here to download high resolution image

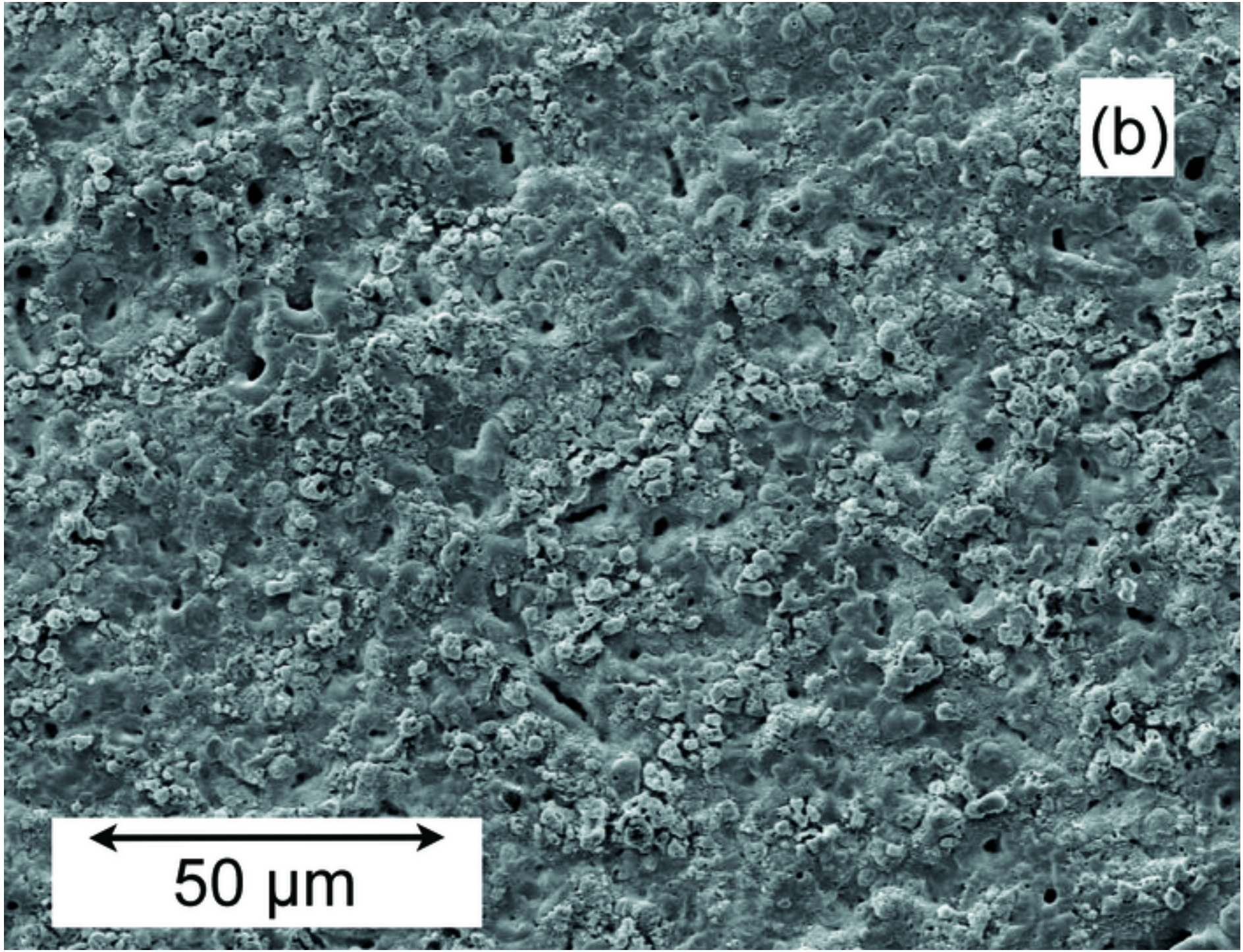

Figure

Click here to download high resolution image

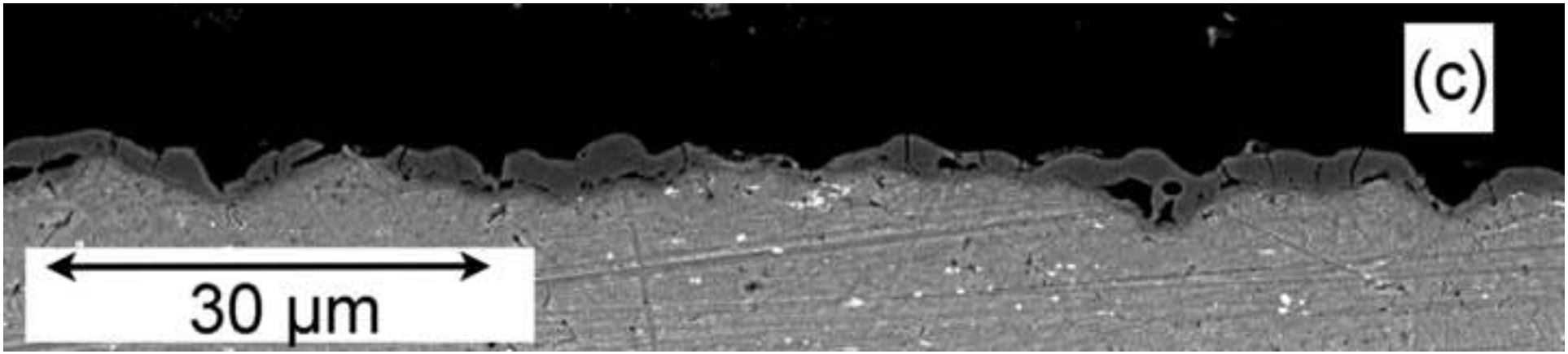

Figure

Click here to download high resolution image

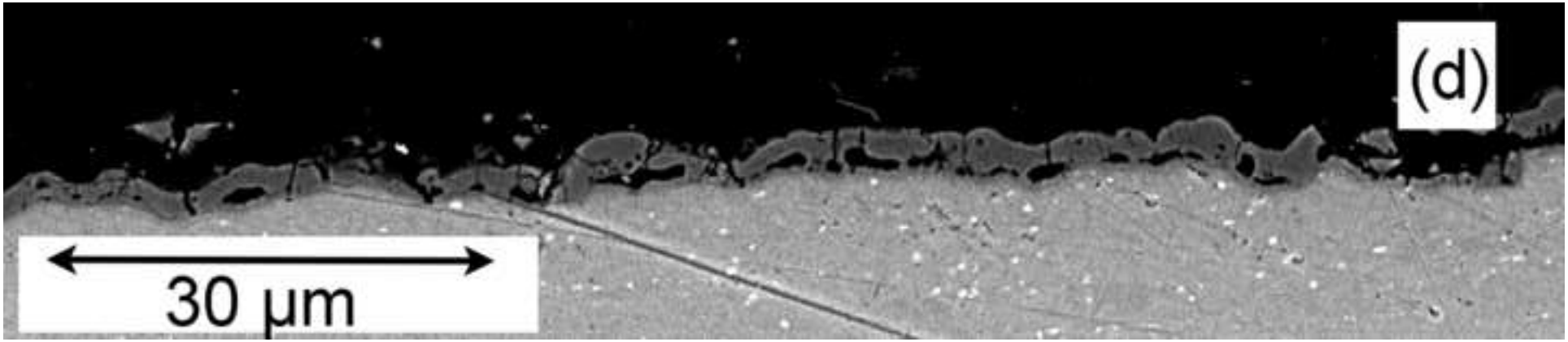

Figure

Click here to download high resolution image

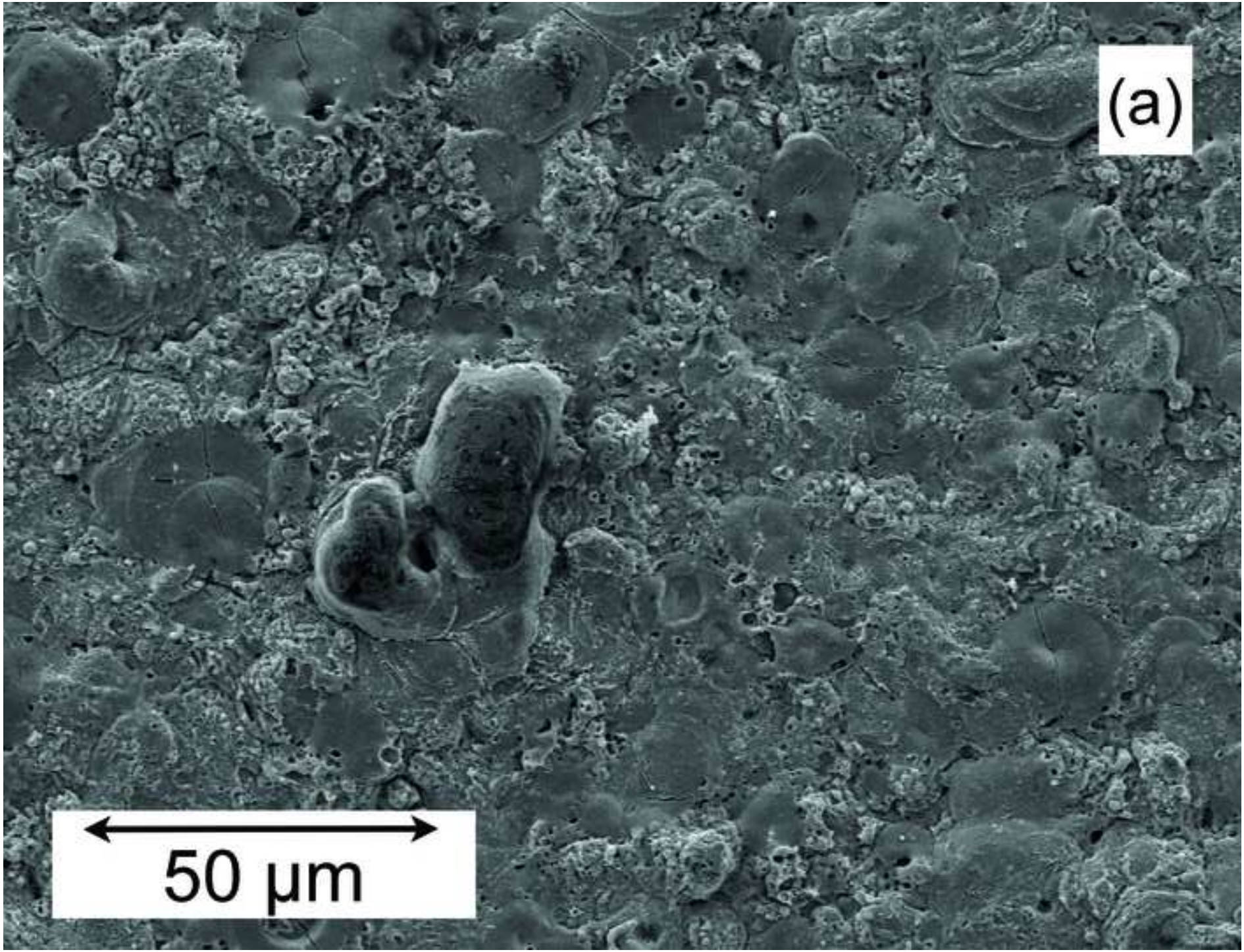

Figure

Click here to download high resolution image

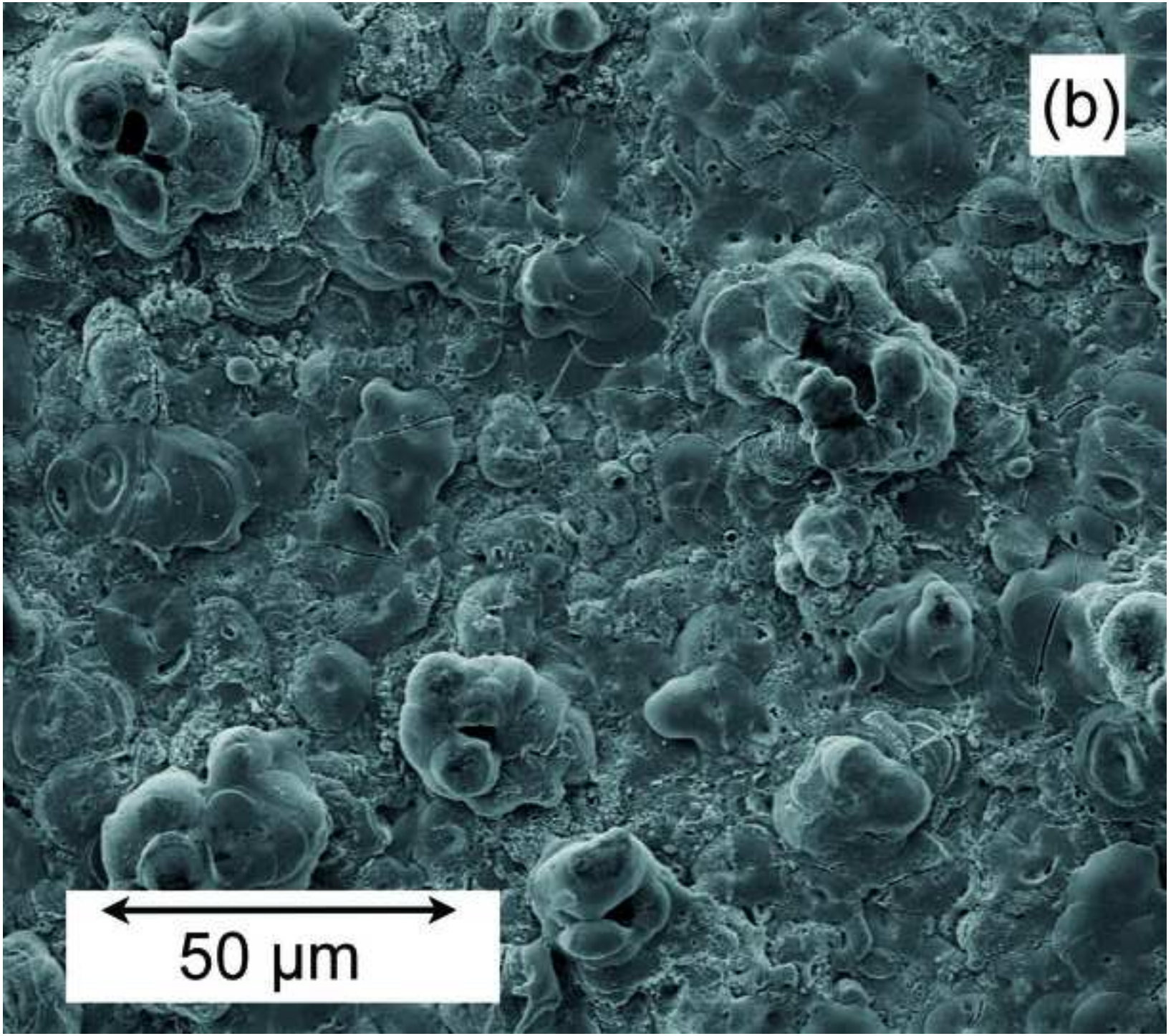

Figure

Click here to download high resolution image

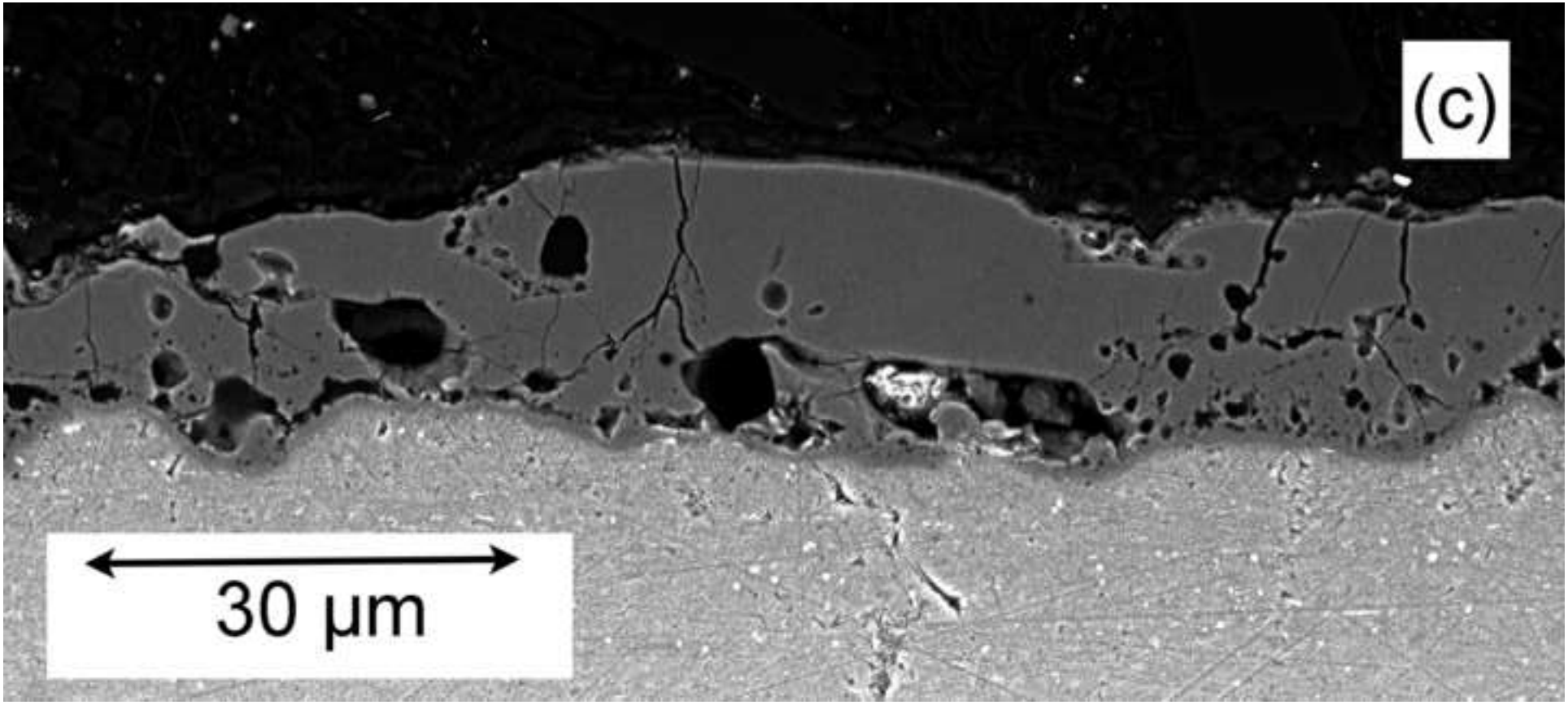

Figure

Click here to download high resolution image

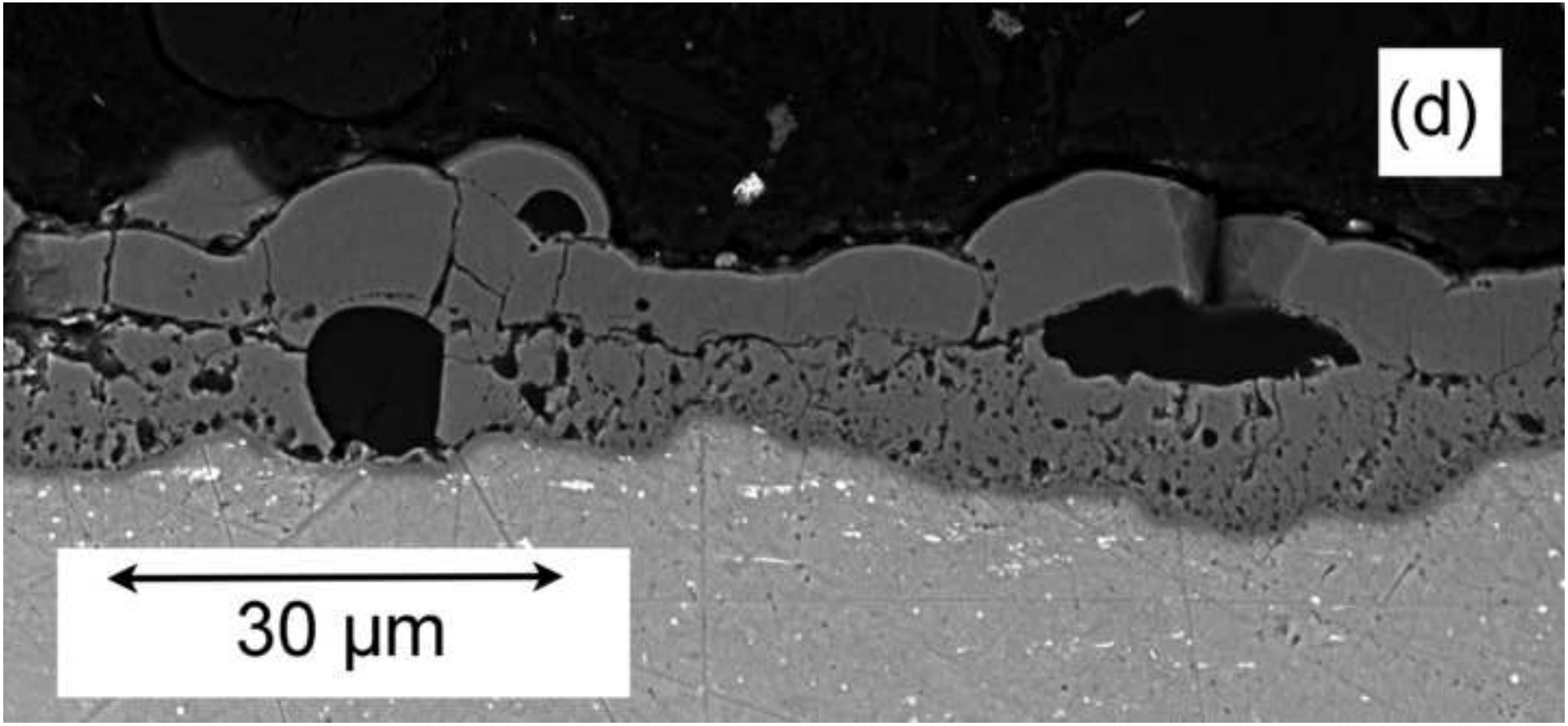

Figure

Click here to download high resolution image

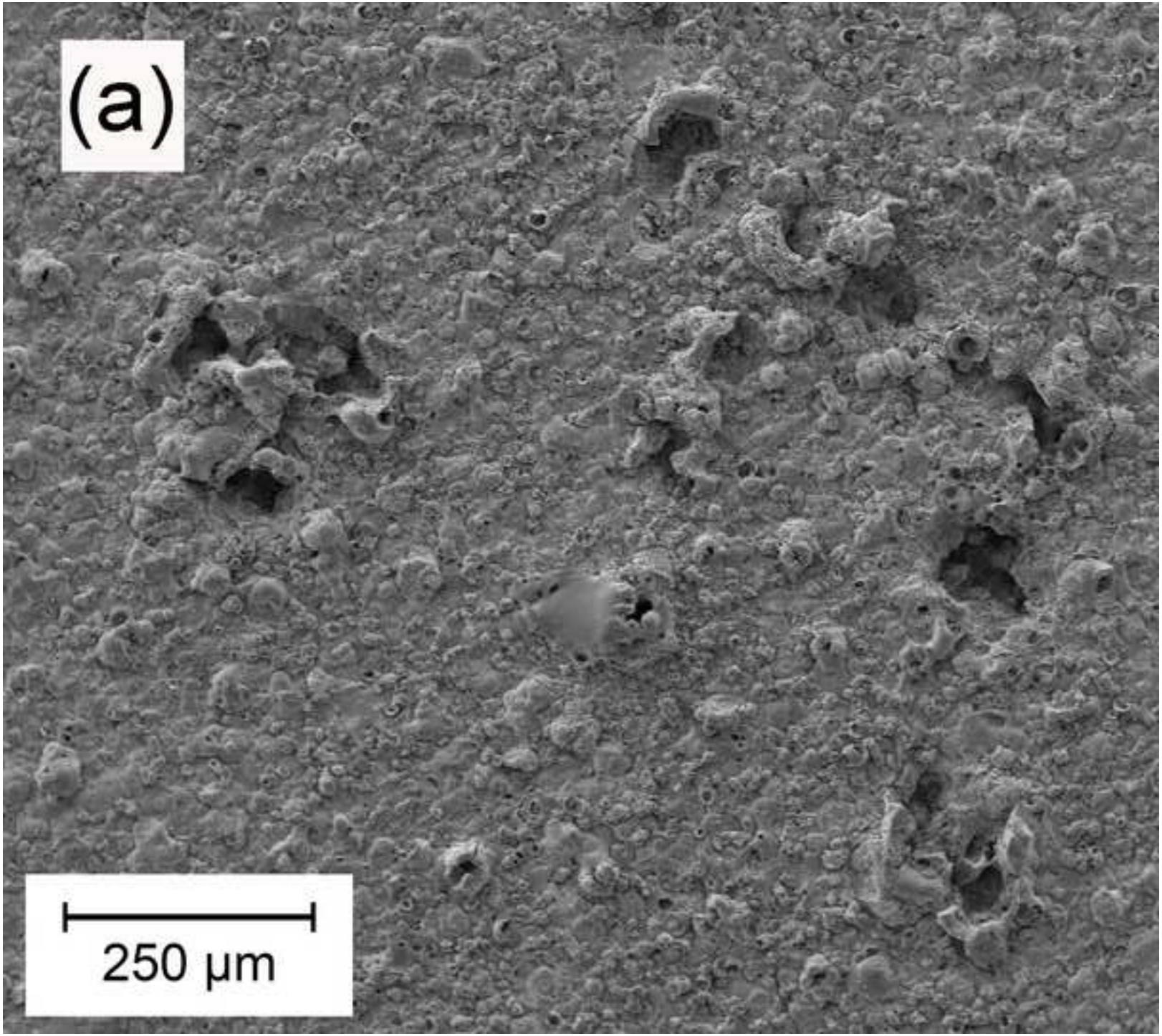

Figure
Click here to download high resolution image

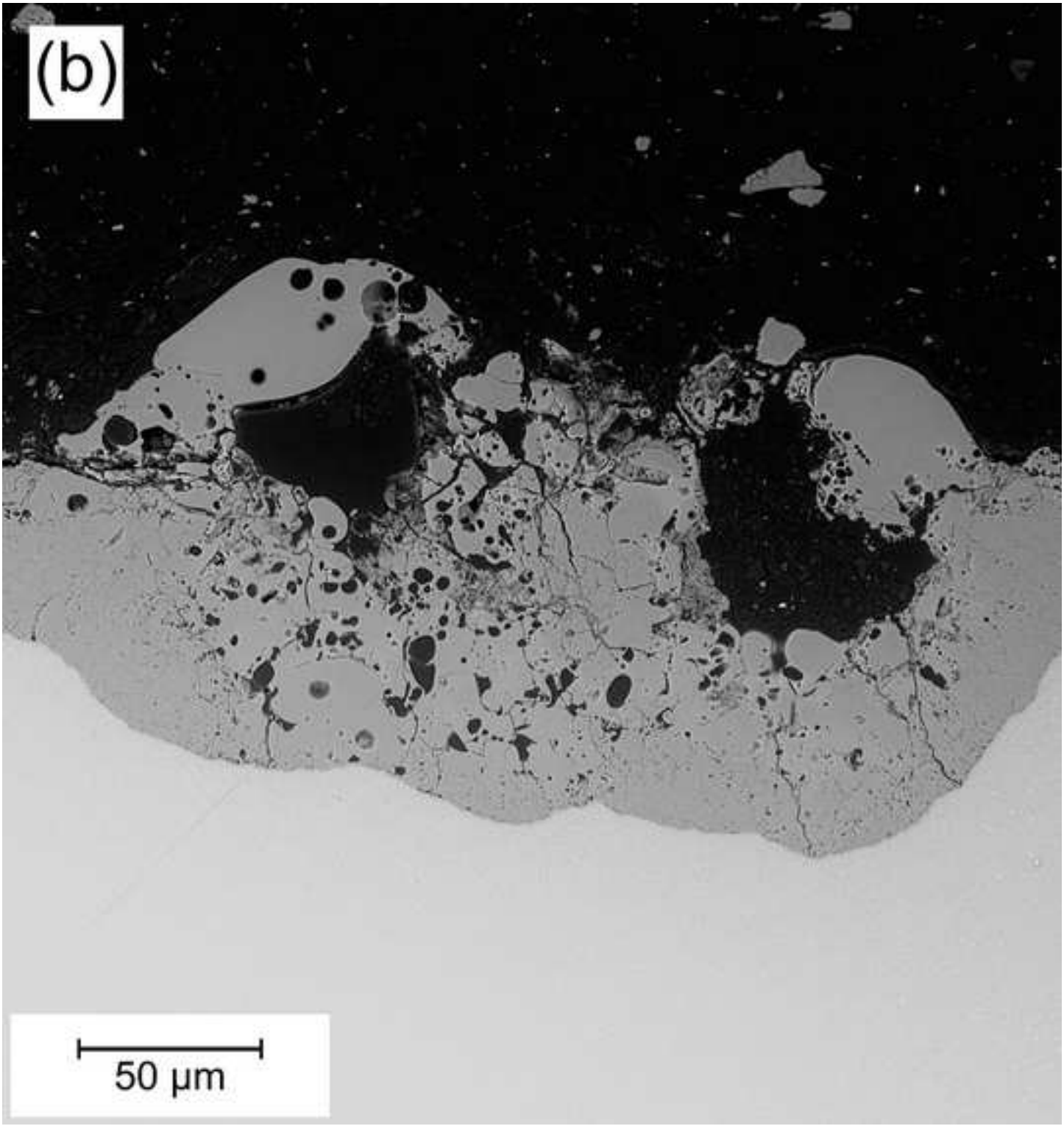

Figure

Click here to download high resolution image